

A transitional species of *Daspletosaurus* Russell, 1970 from the Judith River Formation of eastern Montana (#75847)

1

First revision

Guidance from your Editor

Please submit by **9 Oct 2022** for the benefit of the authors .



Structure and Criteria

Please read the 'Structure and Criteria' page for general guidance.



Custom checks

Make sure you include the custom checks shown below, in your review.



Author notes

Have you read the author notes on the [guidance page](#)?



Raw data check

Review the raw data.



Image check

Check that figures and images have not been inappropriately manipulated.

Privacy reminder: If uploading an annotated PDF, remove identifiable information to remain anonymous.

Files

Download and review all files from the [materials page](#).

1 Tracked changes manuscript(s)

1 Rebuttal letter(s)

13 Figure file(s)

1 Raw data file(s)

1 Other file(s)

! Custom checks

New species checks



Have you checked our [new species policies](#)?



Do you agree that it is a new species?



Is it correctly described e.g. meets ICZN standard?



Structure and Criteria

Structure your review

The review form is divided into 5 sections. Please consider these when composing your review:

1. BASIC REPORTING
2. EXPERIMENTAL DESIGN
3. VALIDITY OF THE FINDINGS
4. General comments
5. Confidential notes to the editor

You can also annotate this PDF and upload it as part of your review

When ready [submit online](#).

Editorial Criteria

Use these criteria points to structure your review. The full detailed editorial criteria is on your [guidance page](#).

BASIC REPORTING

- Clear, unambiguous, professional English language used throughout.
- Intro & background to show context. Literature well referenced & relevant.
- Structure conforms to [Peerj standards](#), discipline norm, or improved for clarity.
- Figures are relevant, high quality, well labelled & described.
- Raw data supplied (see [Peerj policy](#)).

EXPERIMENTAL DESIGN

- Original primary research within [Scope of the journal](#).
- Research question well defined, relevant & meaningful. It is stated how the research fills an identified knowledge gap.
- Rigorous investigation performed to a high technical & ethical standard.
- Methods described with sufficient detail & information to replicate.

VALIDITY OF THE FINDINGS

- Impact and novelty not assessed. *Meaningful* replication encouraged where rationale & benefit to literature is clearly stated.
- All underlying data have been provided; they are robust, statistically sound, & controlled.
- Conclusions are well stated, linked to original research question & limited to supporting results.



The best reviewers use these techniques

Tip

Example

Support criticisms with evidence from the text or from other sources

Smith et al (J of Methodology, 2005, V3, pp 123) have shown that the analysis you use in Lines 241-250 is not the most appropriate for this situation. Please explain why you used this method.

Give specific suggestions on how to improve the manuscript

Your introduction needs more detail. I suggest that you improve the description at lines 57- 86 to provide more justification for your study (specifically, you should expand upon the knowledge gap being filled).

Comment on language and grammar issues

The English language should be improved to ensure that an international audience can clearly understand your text. Some examples where the language could be improved include lines 23, 77, 121, 128 - the current phrasing makes comprehension difficult. I suggest you have a colleague who is proficient in English and familiar with the subject matter review your manuscript, or contact a professional editing service.

Organize by importance of the issues, and number your points

1. Your most important issue
2. The next most important item
3. ...
4. The least important points

Please provide constructive criticism, and avoid personal opinions

I thank you for providing the raw data, however your supplemental files need more descriptive metadata identifiers to be useful to future readers. Although your results are compelling, the data analysis should be improved in the following ways: AA, BB, CC

Comment on strengths (as well as weaknesses) of the manuscript

I commend the authors for their extensive data set, compiled over many years of detailed fieldwork. In addition, the manuscript is clearly written in professional, unambiguous language. If there is a weakness, it is in the statistical analysis (as I have noted above) which should be improved upon before Acceptance.

A transitional species of *Daspletosaurus* Russell, 1970 from the Judith River Formation of eastern Montana

Elías A Warshaw ^{Corresp., 1, 2}, Denver W Fowler ¹

¹ Badlands Dinosaur Museum, Dickinson, North Dakota, United States

² Department of Earth Sciences, Montana State University, Bozeman, MT, United States

Corresponding Author: Elías A Warshaw
Email address: warshawelias@gmail.com

Here we describe a new derived tyrannosaurine, *Daspletosaurus wilsoni* sp. nov., from Judithian strata (~76.5 Ma) intermediate in age between either of the previously described species of this genus. *D. wilsoni* displays a unique combination of ancestral and derived characteristics, including a cornual process of the lacrimal reduced in height relative to *D. torosus* and more basal tyrannosaurines, and a prefrontal with a long axis oriented more rostrally than in *D. horneri* and more derived tyrannosaurines. The description of this taxon provides insight into evolutionary mode in Tyrannosaurinae, lending strength to previous hypotheses of anagenesis within *Daspletosaurus* and increasing the resolution with which the evolution of this lineage can be reconstructed. Cladistic phylogenetic methods, stratigraphy, and qualitative analysis of the morphology of relevant taxa supports an anagenetic model for the origin of morphological novelty in this genus, highlighting the predominance of anagenetic evolution among contemporary dinosaur lineages.

1 **A transitional species of *Daspletosaurus* Russell, 1970 from the Judith** 2 **River Formation of eastern Montana**

3 Elías A. Warshaw^{1,2} and Denver W. Fowler¹

4 1. Badlands Dinosaur Museum, Dickinson Museum Center, Dickinson, North Dakota, USA

5 2. Department of Earth Sciences, Montana State University, Bozeman, Montana, USA

6 Corresponding author:

7 Elías A. Warshaw^{1,2}

8 2137 S 11th Ave 126B, Bozeman, Montana, 59715, USA

9 Email address: warshawelias@gmail.com

10 **Abstract**

11 Here we describe a new derived tyrannosaurine, *Daspletosaurus wilsoni* sp. nov., from
12 Judithian strata (~76.5 Ma) intermediate in age between either of the previously described
13 species of this genus. *D. wilsoni* displays a unique combination of ancestral and derived
14 characteristics, including a cornual process of the lacrimal reduced in height relative to *D.*
15 *torosus* and more basal tyrannosaurines, and a prefrontal with a long axis oriented more
16 rostrally than in *D. horneri* and more derived tyrannosaurines. The description of this taxon
17 provides insight into evolutionary mode in Tyrannosaurinae, lending strength to previous
18 hypotheses of anagenesis within *Daspletosaurus* and increasing the resolution with which the
19 evolution of this lineage can be reconstructed. Cladistic phylogenetic methods, stratigraphy,
20 and qualitative analysis of the morphology of relevant taxa supports an anagenetic model for
21 the origin of morphological novelty in this genus, highlighting the predominance of anagenetic
22 evolution among contemporary dinosaur lineages.

23 **Introduction**

24 Since their naming at the turn of the 20th century, tyrannosaurids have captivated public
25 and scientific imagination alike, and are as a result among the best-studied groups of
26 Cretaceous theropods (Osborn, 1905; Brusatte et al., 2010). Perhaps the most successful group
27 of tyrannosaurids were the latest-Cretaceous tyrannosaurines, including among them a diverse
28 array of forms from the slender-snouted alioramins (Lü et al., 2014) to robust and deep-jawed
29 taxa like *Teratophoneus* (Carr et al., 2011) and the eponymous *Tyrannosaurus rex* (Carr and
30 Williamson, 2010). However, much of the diversity of derived tyrannosaurines remains
31 understudied or poorly understood (Paulina Carabajal et al., 2021), hampering understanding of
32 paleobiogeographic and evolutionary trends (Loewen et al., 2013; Carr et al., 2017; Brusatte
33 and Carr, 2016).

34 The tyrannosaurine *Daspletosaurus* has been known from Campanian fossil deposits of
35 northern Laurasia for over half a century. However, published work on the phylogeny and
36 paleobiology of this genus is relatively scarce beyond its initial description (Russell, 1970; Carr

37 et al., 2017; Paulina Carabajal et al., 2021). Several enigmatic tyrannosaurine specimens initially
38 referred to the type species or simply to *Daspletosaurus* sp. (including the recently named *D.*
39 *horneri*) have been noted as representing novel species by previous workers for several
40 decades (Currie, 2003; Carr, 1999; Carr et al., 2017; Horner et al., 1992; Paulina Carabajal et al.,
41 2021), indicating a more speciose genus than has currently been described. Filling this gap is
42 especially pertinent to understanding rates and patterns of speciation in the Campanian of
43 Laurasia, both within tyrannosaurs and among dinosaurs as a whole, as both described species
44 of *Daspletosaurus* have been hypothesized to represent an anagenetic lineage (Carr et al.,
45 2017), including this genus among the many contemporary dinosaur lineages for which
46 anagenesis has been suggested (Horner et al., 1992; Fowler and Freedman Fowler, 2020).

47 Here we describe *Daspletosaurus wilsoni* (sp. nov.). This addition to Campanian
48 tyrannosaurid diversity has the potential to refine existing hypotheses regarding tyrannosaurid
49 evolution in the Late Cretaceous, and lends strength to the hypothesis of anagenesis as a
50 predominant mode of evolution in *Daspletosaurus* (Carr et al., 2017).

51 Tyrannosaurinae Matthew and Brown, 1922 (*sensu* Sereno et al., 2005)

52 *Daspletosaurus* Russell, 1970

53 *D. wilsoni* sp. nov.

54 Etymology

55 *wilsoni*, Latinization of “Wilson,” after John Wilson, the discoverer of the holotype specimen.

56 Holotype

57 BDM 107, preserving a partial disarticulated skull and jaws, including both premaxillae, a right
58 maxilla, jugal, lacrimal, quadrate, quadratojugal, and dentary, and a left postorbital and
59 squamosal, and missing the braincase, nasals, palate, and every postdentary bone except for a
60 right splenial. Also preserved are partial cervical, sacral, and caudal series, a rib, a chevron, and
61 a first metatarsal. Cranial bones are very finely preserved, with intricate and detailed surface
62 textures especially on the maxilla and postorbital, with teeth preserved in the maxilla, dentary,
63 and one premaxilla. The sacral and caudal centra are preserved in a heavy and hard concretion
64 and are not yet prepared. The holotype specimen is stored in the collections of the Badlands
65 Dinosaur Museum in Dickinson, North Dakota.

66 Geological Setting

67 The site “Jack’s B2” was discovered in 2017 by John Wilson in exposures of the Judith
68 River Formation near Glasgow (Valley County, Montana, USA). This is significantly further east
69 than classic ‘Judith’ localities (Fig. 1), and is sedimentologically atypical, representing distal
70 floodplain and delta sediments deposited during the maximum Campanian regression of the
71 Western Interior Seaway. Here, the Judith River Formation is up to ~48m thick, with the “Jack’s
72 B2” site occurring ~30m below the contact with the overlying Bearpaw Shale.

73 Precise stratigraphic placement of this easternmost Judith is currently unclear, although
74 an age of ~76.5 Ma seems most likely, which would correlate in time with the lower to middle

75 part of the Dinosaur Park Formation, Alberta (Eberth, 2005; Fowler, 2017). A youngest age limit
76 of 75.64 Ma (Ogg & Hinnov, 2012) is delineated by ammonites tentatively identified as
77 *Didymoceras stevensoni* (J. Slattery, pers. comm. 2020) collected by BDM from local outcrops of
78 the overlying Bearpaw Shale (although these were not at the base of the Bearpaw, so older
79 ammonite specimens may be encountered during future prospecting). At present, more precise
80 stratigraphic position can be inferred from the timing of the maximum regression of the
81 Western Interior Seaway during the Campanian (correlated with the R8 regression of
82 Kaufmann, 1977; Rogers et al., 2016). In Alberta and Saskatchewan, the Foremost, Oldman, and
83 Dinosaur Park formations represent early to late subcycles (respectively) of the R8 regression,
84 and of these, the Foremost (~80.5-79.5 Ma) and lower Oldman (~79.5-79.0 Ma; and regional
85 equivalents) are restricted to the west (Alberta and west central Montana), and did not extend
86 as far east as Saskatchewan or our study area in eastern Montana (Eberth, 2005). During late
87 R8, the upper Oldman (~77.5-77.0 Ma) and Dinosaur Park (~76.9-76.0 Ma) Formations were
88 deposited much further to the east, with the lowermost Dinosaur Park recording the R8
89 maximum regression at ~76.9 - 76.4 Ma (Eberth, 2005; Fowler, 2017). This correlates well with
90 the Judith River Formation of Montana, where Rogers et al. (2016) show the maximum
91 regression of R8 occurring shortly before 76.2 Ma, based on radiometric dates acquired either
92 side of the mid-Judith discontinuity. As such, it seems likely that the study section corresponds
93 in age to the lower to middle part of the Dinosaur Park Formation (although not necessarily
94 lithostratigraphically correlated). A radiometric analysis of a newly discovered volcanic ash is
95 currently underway, and it is hoped that this will provide definitive stratigraphic placement.

96 Regardless of the precise age of BDM 107, it can be expected to lie intermediate
97 stratigraphically between *D. torosus* (known from the upper Oldman Formation, ~77.0 Ma;
98 Carabaja et al., 2021) and *D. horneri* (known from the Two Medicine Formation, ~75.0 Ma; Carr
99 et al., 2017).

100 Diagnosis

101 *D. wilsoni* can be assigned to *Daspletosaurus* based on the following characteristics:
102 extremely coarse subcutaneous surface of the maxilla with no elevated ridges or corresponding
103 fossae (Carr et al., 2017; Voris et al., 2020); cornual process of the postorbital approaching the
104 laterotemporal fenestra (Carr et al., 2017); dorsal postorbital process of the squamosal
105 terminating caudal to the rostral margin of the laterotemporal fenestra (Carr et al., 2017; Voris
106 et al., 2019); and extremely coarse symphyseal surface of the dentary (Voris et al., 2020).

107 *D. wilsoni* lacks autapomorphies and can be diagnosed by a unique combination of
108 ancestral and derived *Daspletosaurus* characteristics. *D. wilsoni* and *D. torosus* share a
109 pneumatic inflation of the lacrimal reaching the medial edge of the bone (this inflation does not
110 reach the medial edge of the bone in the holotype of *D. horneri*, but this may represent an
111 allometric, ontogenetic, or taphonomic bias; see Warshaw, In Review; Carr et al., 2017),
112 prefrontal oriented rostromedially (determined from the angle of the prefrontal articular
113 surface on the lacrimal of the holotype of *D. wilsoni*, which does not preserve a prefrontal; the
114 prefrontal of *D. horneri* is oriented mediolaterally), pneumatic excavation of the squamosal that
115 does not undercut its rostromedial margin (entire margin undercut in *D. horneri*; Carr et al.,
116 2017), and quadratojugal lacking a pneumatic foramen in its lateral surface (although the

117 presence of this foramen is highly intraspecifically variable in both *D. horneri* and
118 *Tyrannosaurus*, such that further discoveries of *D. wilsoni* individuals may reveal its presence in
119 this taxon; Carr et al., 2017; Carr, 2020). *D. horneri* and *D. wilsoni* share, to the exclusion of *D.*
120 *torosus*, a premaxillary tooth row oriented entirely mediolaterally, such that all but one
121 premaxillary tooth is concealed in lateral view (rostromedial orientation in *D. torosus* and less
122 derived tyrannosaurids), antorbital fossa of the maxilla terminating at the rostral limit of the
123 external antorbital fenestra (this fossa extends ahead of this boundary onto the subcutaneous
124 surface of the maxilla in *D. torosus* and less derived tyrannosaurids; Carr et al., 2017; Warshaw,
125 In Review), rostradorsal ala of the lacrimal inflated (uninflated in *D. torosus* and less derived
126 tyrannosaurids), ventral ramus of the lacrimal longer than the rostral ramus (determined largely
127 by the height of the postorbital bar in the reconstructed skull, given that the ventral ramus is
128 largely unpreserved in the holotype of *D. wilsoni*; the rostral ramus of the lacrimal is longer
129 than the ventral ramus in *D. torosus*; Carr et al., 2017), short cornual process of the lacrimal (tall
130 in *D. torosus*, although this process is taller in *D. wilsoni* than *D. horneri* and may best be
131 described as intermediate between the previously named species of this genus; Carr et al.,
132 2017), and dorsal quadrate contact of the quadratojugal visible in lateral view (concealed in *D.*
133 *torosus* and less derived tyrannosaurids).

134 Description

135 Given the wealth of detailed osteologies describing tyrannosaurine specimens (i.e.,
136 Brochu, 2003; Hurum and Sabath, 2003; Carr, 1999), our description of the holotype of *D.*
137 *wilsoni* places heavy emphasis on characteristics (or combinations of characteristics) unique to
138 this specimen, as well as those that are otherwise taxonomically or phylogenetically informative
139 within Tyrannosaurinae, so as to avoid the reiteration of plesiomorphic tyrannosaurine
140 morphologies (or synapomorphies of *Daspletosaurus*) already described by previous authors.

141 Ontogenetic Stage of BDM 107

142 In order to facilitate comparison with other tyrannosaurine individuals of equivalent
143 ontogenetic stages (and in doing so, to avoid the misattribution of a phylogenetic signal to
144 ontogenetically derived characteristics), brief comment is warranted on the ontogenetic stage
145 represented by BDM 107; two lines of evidence suggest that this specimen is of advanced
146 ontogenetic age. Firstly, BDM 107 is among the largest known *Daspletosaurus* individuals
147 (reconstructed skull length 105 cm; *D. torosus* holotype CMN 8506 skull length 104 cm, Voris et
148 al., 2019; *D. horneri* holotype MOR 590 skull length 89.5 cm, Carr et al., 2017). Although Carr
149 (2020) criticized the use of size as an indicator of ontogenetic status in *Tyrannosaurus*, this
150 criticism was based on the absence of a correlation between size and maturity among adult
151 individuals; all the largest specimens of this genus were unambiguously recovered as adult by
152 Carr's (2020) analysis (i.e., within the final stages of ontogenetic development), such that this
153 feature remains ontogenetically informative in distinguishing adults from juveniles and
154 subadults. Secondly, BDM 107 displays several morphologies known otherwise to characterize
155 mature tyrannosaurines, including a deeply scalloped maxilla-nasal suture (Carr and
156 Williamson, 2004; Carr, 2020), a maxillary fenestra positioned rostrally within the antorbital
157 fossa (Carr, 2020), a cornual process of the lacrimal inflated and positioned dorsal to the ventral
158 ramus (Carr, 1999; Currie, 2003; Carr, 2020), and a grossly exaggerated cornual process of the

159 postorbital (Carr, 1999; Currie, 2003; Voris et al., 2019; Carr, 2020). The totality of this evidence
160 supports an adult ontogenetic stage or later for BDM 107 (adult *sensu* Carr 2020; ontogenetic
161 Stage 4 *sensu* Carr, 1999); this hypothesis may be tested in future work through histological
162 analysis and/or comparison with further discoveries of *D. wilsoni* individuals of different
163 ontogenetic stages, both of which lie outside of the scope of the present study.

164 *Premaxilla*

165 The premaxillae of *D. wilsoni* are similar to those of *D. horneri*, *Tarbosaurus*, and
166 *Tyrannosaurus* in that the alveolar row is oriented largely mediolaterally, such that the rostrum
167 of the skull is broad and the labial surfaces of the premaxillary teeth face rostrally (Brochu,
168 2003, Fig. 4; Hurum and Sabbath, 2003, Fig. 3; Carr et al., 2017, Fig. 1; Fig. 2). In *Tyrannosaurus*
169 and similarly derived tyrannosaurines (*Tarbosaurus* and *D. horneri*), the premaxillary teeth
170 largely overlap each other in lateral view such that only the distalmost tooth is clearly visible;
171 the same would be true of the holotype of *D. wilsoni*, were more than a single premaxillary
172 tooth preserved within its socket. Conversely, the premaxillary tooth row of *D. torosus* and less
173 derived tyrannosauroids is oriented rostromedially, such that multiple teeth are clearly visible
174 in lateral view (Voris et al., 2019, Fig. 6).

175 Although previous authors have regarded a mediolaterally oriented premaxillary tooth
176 row as a synapomorphy of Tyrannosauridae or more inclusive groups (e.g., Carr et al., 2017:
177 character 15), this is in error; mature specimens of *Gorgosaurus* (UALVP 10, Voris et al., 2022,
178 Fig. 1; AMNH 5458, Matthew and Brown, 1923, Fig. 2) and *Qianzhousaurus* (GM F10004, Foster
179 et al., 2022, Fig. 2), have rostromedially oriented premaxillary tooth rows such that in
180 specimens with preserved teeth, all premaxillary teeth are visible in lateral view (although all
181 tyrannosaurids do have premaxillary tooth rows oriented more medially than basal
182 tyrannosauroids; this is the phylogenetic signal recorded in character 15 of Carr et al., 2017).
183 Comparison with other tyrannosaurids is hampered by the absence of preserved premaxillae
184 and/or published descriptions of this element for several species (e.g., *Thanatotheristes*,
185 *Dynamoterror*, *Nanuqsaurus*, *Lythronax*, and *Teratophoneus*, for which all published specimens
186 lack premaxillae; Voris et al., 2020; McDonald, Wolfe, and Dooley, 2018; Fiorillo and Tykoski,
187 2014; Loewen et al., 2013); however, *D. wilsoni* and more derived tyrannosaurines (*D. horneri*,
188 *Tarbosaurus*, *Tyrannosaurus*) represent the greatest exaggeration of the medial inclination of
189 the premaxillary tooth row among tyrannosaurids for which comparative material is available
190 (although this condition, with only one clearly visible premaxillary tooth in lateral view, is
191 present in at least one *Gorgosaurus*: TCM1 2001.89.1, Voris et al., 2022, Fig. 10). *D. torosus* is
192 intermediate between the (presumably) ancestral rostromedial orientation and the
193 mediolateral condition of later *Daspletosaurus* species; two to three premaxillary teeth are
194 visible in lateral view in the holotype specimen, CMN 8506 (Carr and Williamson, 2004, Fig. 6;
195 Voris et al., 2019, Fig. 6).

196 It should be noted that the orientation of the premaxillary tooth row is not necessarily
197 equivalent to the orientation of the premaxillae themselves. In *Tyrannosaurus* AMNH 5027, for
198 example, the premaxillae appear to be rostromedially oriented in dorsal view (Carr and
199 Williamson, 2004, Fig. 7); however, the premaxillary alveoli are mediolaterally arranged when
200 viewed ventrally (EW, pers. obs.; Molnar, 1991, Fig. 9A; Osborn, 1912, Fig. 5A).

201 The taxonomic utility of this character is a hypothesis that will require further testing as
202 individuals of *D. wilsoni* and other tyrannosaurids with preserved premaxillae are discovered;
203 notably, two specimens previously referred to *D. torosus* display the derived condition
204 (mediolateral orientation), sharing it with *D. wilsoni* and more derived tyrannosaurines: FMNH
205 PR308 (Matthew and Brown, 1923, Fig. 5; Carr, 1999, Fig. 1) and TMP 2001.36.1 (Voris et al.,
206 2019, Fig. 6). If these individuals were to represent *D. torosus*, the distinction between this
207 species and *D. wilsoni* in the orientation of the premaxillary tooth row would be heavily
208 undermined; however, both of these specimens have previously been noted as belonging to a
209 novel taxon from the Dinosaur Park Formation (FMNH PR308, Currie, 2003; TMP 2001.36.1,
210 Carabajal et al., 2021). Therefore, although relevant comparisons will be made with these
211 specimens hereafter, they will be considered separately from *D. torosus* (and will be referred to
212 below as the Dinosaur Park taxon). A precise taxonomic designation for these specimens is
213 reserved for future work in accordance with comments by previous authors (Currie, 2003;
214 Carabajal et al., 2021).

215 There is a small (~2 cm diameter) indentation in the nasal process of the right premaxilla
216 of BDM 107; this is most likely pathological, as it is irregular in form and not present on the left
217 premaxilla.

218 *Maxilla*

219 As in other *Daspletosaurus*, the subcutaneous surface of the maxilla in *D. wilsoni* is
220 densely covered in anastomosing sulci extending from neurovascular foramina (Carr et al.,
221 2017; Voris et al., 2020; Fig. 3). The degree of sculpturing of this surface in BDM 107 is similar to
222 CMN 8506 (*D. torosus*), although in the former, there is no smooth region rostral to the
223 external antorbital fenestra indicating a rostral continuation of the antorbital fossa as *D.*
224 *torosus* and alioramins (Carr et al., 2017). As in *Thanatotheristes* and other *Daspletosaurus*
225 species, the shallow excavations that characterize the maxillae of the most derived
226 tyrannosaurines (*Zhuchengtyrannus*, *Tyrannosaurus*, *Tarbosaurus*; Hone et al., 2011; Voris et
227 al., 2020) are absent from the holotype maxilla of *D. wilsoni*. Also absent are the textural ridges
228 present on the maxillae of *Thanatotheristes*, *Zhuchengtyrannus*, *Tarbosaurus*, and
229 *Tyrannosaurus* but not any *Daspletosaurus* species (Hone et al., 2011; Voris et al., 2020).

230 The rostral end of the maxilla of BDM 107 is bowed subtly medially towards its contact
231 with the premaxilla and nasal; this may be a structural consequence of the greater medial
232 inclination of the premaxillary tooth row (see above), as a similar condition characterizes *D.*
233 *horneri* (MOR 590, EW, pers. obs.), *Tarbosaurus* (Hurum and Sabbath, 2003, Fig. 15), and
234 *Tyrannosaurus* (MOR 008, MOR 980, EW, pers. obs.). Tyrannosaurids with more rostromedially
235 inclined premaxillary tooth rows lack this bowing (e.g., *D. torosus* CMN 8506, JT Voris, pers.
236 comm., 2022).

237 The maxilla of BDM 107 is irregular relative to other species of *Daspletosaurus* in that it
238 is proportionally elongate, being 64.1 cm in length and 24.8 cm in height (ratio of length to
239 height = 2.6). This bone is 58.6 cm long rostrocaudally and 27.5 cm tall dorsoventrally in the
240 holotype of *D. horneri* (ratio of length to height = 2.1; MOR 590, Carr et al., 2017). Given the
241 broad range of variation in the proportions of this element in other tyrannosaurine species for

242 which larger sample sizes are known (e.g., *Tyrannosaurus*; Carpenter, 1990; Paul, Persons, and
243 Van Raalte, 2022; pers. obs., EW), this characteristic was not included as an autapomorphy of *D.*
244 *wilsoni*. Consistency in this trait across further discoveries of *D. wilsoni* individuals may require
245 a reevaluation of the taxonomic utility of this character.

246 *D. wilsoni* possesses 15 maxillary alveoli, as in other species of *Daspletosaurus* (Carr et
247 al., 2017). The 13th alveolus bears a swollen abscess in BDM 107, and the 15th maxillary tooth
248 conceals a small replacement tooth within its root that is visible in medial (lingual) view. In
249 general, the maxillary teeth are similar to those of other tyrannosaurid species in being
250 labiolingually broad, although not to the degree present in more derived tyrannosaurines (e.g.,
251 *Tyrannosaurus* and *Tarbosaurus*), in which the labiolingual width of the maxillary teeth is
252 subequal to their mesiodistal length (Carr et al., 2017). The first maxillary alveolus is not small
253 and also bears an incassate tooth (i.e., it does not bear a d-shaped crown similar to those
254 present in the premaxillae, as in *Gorgosaurus*; Currie et al., 2003; Voris et al., 2022).

255 *Jugal*

256 The jugal of *D. wilsoni* is most similar to that of *D. torosus* among tyrannosaurines in
257 that it has a mediolaterally thin ventral margin of the orbit (as opposed to a rounded margin as
258 in *Thanatotheristes*, *Lythronax*, most *Tarbosaurus*, and some *Tyrannosaurus*; Voris et al., 2020;
259 Voris et al., 2022; JT Voris, pers. comm., 2022. A thin ventral margin of the orbit likely
260 represents the ancestral tyrannosaurid condition, as it is also present in *Bistahieversor*,
261 *Albertosaurus*, *Gorgosaurus*, and *D. horneri*; JT Voris, pers. comm., 2022) and does not bow
262 medially along its rostrocaudal length (the jugals of *D. horneri*, *Tyrannosaurus*, and *Tarbosaurus*
263 are angled rostromedially rostral to the orbit, such that the maxillae are medially inset from the
264 orbitotemporal region; *D. horneri* MOR 590, EW, pers. obs.; *Tyrannosaurus* AMNH 5027,
265 Molnar, 1991, Fig. 9; *Tarbosaurus* GIN 107/1, Hurum and Sabbath, 2003, Fig. 15; Warshaw, In
266 Review).

267 As in *D. torosus*, the caudal portion of the lacrimal contact surface of the jugal is
268 shallowly inclined (Fig. 4); this surface is very steep in *D. horneri*, as well as in *Albertosaurus* and
269 *Gorgosaurus* (Carr et al., 2017). Although Carr et al. (2017) recovered this feature as unique to
270 *D. horneri* among tyrannosaurines, it is also present in some *Tyrannosaurus* individuals (MOR
271 980, MOR 1125, AMNH 5027, EW, pers. obs.).

272 *Lacrimal*

273 As in all tyrannosaurids except for *D. horneri*, *Tarbosaurus*, and *Tyrannosaurus*, the
274 cornual process of the lacrimal in *D. wilsoni* is large and rises to a distinct apex along its dorsal
275 margin (Carr et al., 2017; Fig. 5). This apex is situated directly dorsal to the lacrimal's ventral
276 ramus, as is characteristic of mature tyrannosaurines (Currie, 2003; Carr, 2020). The cornual
277 process of the lacrimal is shorter in *D. wilsoni* (5.2 cm from the dorsal margin of the lacrimal
278 antorbital recess to the apex of the cornual process in BDM 107) than *D. torosus* (6.9 cm, CMN
279 8506; Voris et al., 2019, Fig. 6), but similar to the Dinosaur Park taxon (5.1 cm, TMP 2001.36.1;
280 Voris et al., 2019, Fig. 6) (these three specimens are each within 2 cm of each other in skull
281 length, such that measurements of this process need not be corrected for differences in

282 absolute specimen size; see above; Voris et al., 2019, Fig. 6). The lacrimal cornual process of the
283 *D. horneri* holotype MOR 590 is shorter still (3.7 cm; Carr et al., 2017, Fig. 1), although it should
284 be noted that this specimen is also ~15% shorter in skull length than any of the specimens
285 previously mentioned (Carr et al., 2017; Voris et al., 2019; see above), such that the difference
286 in this feature between *D. horneri* and other *Daspletosaurus* is relatively less pronounced than
287 isolated measurements of this process would suggest (scaled isometrically to the same skull
288 length as MOR 590, however, BDM 107 would still have a taller cornual process of the lacrimal,
289 at 4.4 cm).

290 Carr et al. (2017) regarded an accessory cornual process of the lacrimal as a
291 synapomorphy of *Daspletosaurus*. However, this process is indistinguishable from the caudally
292 directed supraorbital process of the lacrimal upon which it is purported to sit; the supraorbital
293 processes of the lacrimals of *Tyrannosaurus* (MOR 555, MOR 980, MOR 1125, AMNH 5027, EW,
294 pers. obs.), *Tarbosaurus* (ZPAL MgD-I/4, Hurum and Sabbath, 2003, Fig. 6), and *Teratophoneus*
295 (UMNH VP 16690, Loewen et al., 2013, Fig. 3) are all morphologically identical to those of
296 *Daspletosaurus*, although they are scored by Carr et al. (2017) as lacking an accessory cornual
297 process. In lieu of any quantitative demonstration of this process's presence in *Daspletosaurus*,
298 the taxonomic utility of this character is rejected here.

299 The lacrimal antorbital recess differs in morphology from *D. torosus*, but is similar to
300 that of *D. horneri*, *Tarbosaurus*, and *Tyrannosaurus* in that the rostradorsal ala joining the
301 rostral and ventral rami of the lacrimal is inflated into a cylindrical bar that is elevated in relief
302 relative to the rest of the recess (this ala is inflated in *D. torosus*, but to a lesser degree such
303 that no discrete bar is formed between the rostral and ventral rami; Carr et al., 2017, Fig. S2F)
304 (EW, pers. obs.). This feature is also present in the Dinosaur Park taxon (TMP 2001.36.1, Voris
305 et al., 2019, Fig. 6). Also distinguishing the lacrimal of *D. wilsoni* from *D. torosus* is a ventrally
306 directed antorbital fossa in the latter. The lacrimal antorbital fossa is laterally directed in other
307 tyrannosaurids, including *D. wilsoni*, the Dinosaur Park taxon (TMP 2001.36.1, Voris et al., 2019,
308 Fig. 6), *D. horneri* (MOR 590 and MOR 1130, Carr et al., 2017, Fig. 3), *Tyrannosaurus*,
309 *Tarbosaurus*, *Albertosaurus*, and *Gorgosaurus* (Carr and Williamson, 2004, Fig. 10).

310 Rostrally, the ventral process of the lacrimal rostral ramus is unique in *D. wilsoni* in
311 having a rounded distal end; this process comes to a pronounced tip in most tyrannosaurids
312 (Carr, Williamson, and Schwimmer, 2005, Fig. 8; Loewen et al., 2013, Fig. 3), with the possible
313 exception of *D. horneri*, in which the holotype specimen MOR 590 has a pointed ventral process
314 and that of the paratype MOR 1130 is rounded (EW, pers. obs.; Carr et al., 2017, Figs. 2C, 3).
315 Given the eminent possibility of taphonomic alteration of this feature (i.e., "rounding down" of
316 a pointed ventral process into a rounded one by abrasion prior to burial), exaggerated by the
317 small size of the ventral process of the lacrimal, this feature is excluded from consideration
318 either as an autapomorphy of *D. wilsoni* or as uniting this species with *D. horneri*.

319 Caudodorsally, the prefrontal articular surface of the lacrimal can be used to determine
320 the orientation of the long axis of the prefrontal. In *D. wilsoni* and *D. torosus*, this element is
321 oriented rostrocaudally (Carr and Williamson, 2004, Fig. 8). This condition is shared with the
322 Dinosaur Park taxon (TMP 2001.36.1, Carabajal et al., 2021, Fig. 2D), and is also present in
323 *Gorgosaurus* (UALVP 10, Voris et al., 2022), *Teratophoneus* (UMNH VP 16690, Loewen et al.,

324 2013, Fig. 3), and *Qianzhousaurus* (GM F10004, Foster et al., 2022, Fig. 3). Conversely, the
325 prefrontal is oriented rostromedially or mediolaterally in *D. horneri* (MOR 590, EW pers. obs.;
326 Carr et al., 2017, Fig. 1), *Tarbosaurus* (ZPAL MgD-I/4, Hurum and Sabbath, 2003, Fig. 1), and
327 *Tyrannosaurus* (AMNH 5027, EW pers. obs.; Carr and Williamson, 2004, Fig. 8), as well as at
328 least one specimen of *Albertosaurus* (TMP 1981.10.1, Carr and Williamson, 2004, Fig. 8).

329 *Postorbital*

330 The postorbital of *D. wilsoni* is most similar to that of *D. torosus* and the Dinosaur Park
331 taxon in bearing a massive cornual process that approaches the rostral margin of the
332 laterotemporal fenestra caudally (Fig. 6; *D. torosus* CMN 8506, Voris et al., 2019, Fig. 6; TMP
333 2001.36.1, Voris et al., 2019, Fig. 4; Carr et al., 2017). Carr et al. (2017) proposed a cornual
334 process of the postorbital approaching the laterotemporal fenestra as a synapomorphy of
335 *Daspletosaurus*; however, the cornual process of the postorbital does not approach the
336 laterotemporal fenestra in the holotype of *D. horneri* (MOR 590, EW pers. obs.), and is instead
337 broadly separated from it as in *Tyrannosaurus* (MOR 980, MOR 1125, MOR 555, EW, pers. obs.)
338 and *Tarbosaurus* (ZPAL MgD-I/4, Hurum and Sabbath, 2003, Fig. 1).

339 Also shared between *D. wilsoni*, *D. torosus*, and the Dinosaur Park taxon is the
340 subdivision of the postorbital cornual process into two discrete processes: a supraorbital shelf
341 protruding from the dorsal margin of the orbit and a caudodorsal tuberosity emerging more
342 caudoventrally (Fig. 6; Voris et al., 2019, Fig. 4D), creating a sinusoidal relief when the
343 postorbital is viewed rostrally or caudally. Both the supraorbital shelf and the caudodorsal
344 tuberosity are situated upon a more 'typical' tyrannosaurine cornual process; that is, they lie
345 lateral to a gross swelling of the postorbital similar to that present in other tyrannosaurines
346 (e.g., *Tyrannosaurus*, MOR 1125, MOR 980, MOR 555, MOR 008, EW, pers. obs.). The
347 caudodorsal tuberosity overhangs its caudoventral base, creating a crease between this process
348 and the underlying body of the postorbital; a similar condition is present in the postorbital
349 cornual processes of *Gorgosaurus*, *Teratophoneus*, and *Bistahieversor* (Voris et al., 2022; JT
350 Voris, pers. comm., 2022), but not in *D. horneri* (MOR 590, Carr et al., 2017, Fig. 1),
351 *Tyrannosaurus* (MOR 1125, MOR 980, MOR 555, MOR 008, EW, pers. obs.), or *Tarbosaurus*
352 (ZPAL MgD-I/4, Hurum and Sabbath, 2003, Fig. 8). A similar crease forms between the body of
353 the postorbital and the cornual process of *Tyrannosaurus* in specimens with an epipostorbital
354 (*sensu* Carr, 2020; AMNH 5027, Molnar 1991; Carr, 2020); however, no such element is present
355 in the holotype of *D. wilsoni* (or any other *Daspletosaurus* specimens; EW, pers. obs.).

356 The ventral ramus of the postorbital tapers ventrally to a point in *D. wilsoni*, as in other
357 *Daspletosaurus* (Carr, 1999), including the Dinosaur Park taxon (Voris et al., 2019, Fig. 4), and in
358 contrast to the enormous subocular process of the postorbital that projects rostrally in
359 *Tyrannosaurus* (Carr, 2020), *Tarbosaurus* (Hurum and Sabbath, 2003, Fig. 8), *Gorgosaurus* (Voris
360 et al., 2022), *Teratophoneus* (Loewen et al., 2013, Fig. 3), and *Albertosaurus* (Currie, 2003).
361 Although the subocular process is present in *D. wilsoni* (and other *Daspletosaurus*), it is small
362 relative to those of other tyrannosaurids (Fig. 6).

363 *Squamosal*

364 The squamosal of *D. wilsoni* is indistinguishable from that of *D. torosus* in that the
365 rostralmost extent of the postorbital contact surface terminates caudal to the rostral margin of
366 the laterotemporal fenestra (also in *D. horneri*; Carr et al., 2017), the rostromedial margin of
367 the pneumatic recess on the ventral surface is not undercut (Fig. 7), and the caudal process is
368 pneumatized (as evidenced by pneumatic foramina in the process's rostromedial surface; Carr
369 et al., 2017). No characteristics or combinations of characteristics unique to *D. wilsoni* are
370 observable on this element.

371 *Quadratojugal*

372 The quadratojugal is conservative morphologically across tyrannosaurids (Loewen et al.,
373 2013). However, a single characteristic of the quadratojugal of *D. wilsoni* unites it with *D.*
374 *horneri* and at least one specimen of the Dinosaur Park taxon (TMP 2001.36.1), and differs from
375 the condition in *D. torosus* and less derived tyrannosaurids: a dorsal quadrate contact that is
376 broadly visible in lateral view. In most tyrannosauroids, the dorsal quadrate contact of the
377 quadratojugal is directed medially or rostromedially such that it is obscured by the body of the
378 quadratojugal in lateral view. In *D. wilsoni*, *D. horneri*, and TMP 2001.36.1, however, this
379 process is directed caudomedially, exposing it laterally (Fig. 8; MOR 590, Carr et al., 2017, Fig. 1;
380 TMP 2001.36.1, Voris et al., 2019, Fig. 6).

381 The dorsal quadrate contact is marginally visible laterally in the holotype of *D. torosus*,
382 CMN 8506 (Voris et al., 2019, Fig. 6; JT Voris, pers. comm., 2022), but not nearly to the extent
383 observable in the aforementioned taxa. The condition in *D. torosus* may therefore represent
384 individual variation on the caudomedial orientation of most tyrannosaurids, or a structural
385 antecedent to the condition present in other species of *Daspletosaurus*.

386 The caudomedial orientation of the dorsal quadrate contact is reversed in the paratype
387 specimen of *D. horneri*, in which this process is hidden in lateral view (MOR 1130, Carr et al.,
388 2017, Fig. S2K). Given that this specimen is younger stratigraphically than the holotype (MOR
389 590; Carr et al., 2017), this reversal may represent a phylogenetic signal (although it may
390 instead represent intraspecific variation). *Tarbosaurus* and *Tyrannosaurus* share this feature
391 with MOR 1130.

392 *Quadrate*

393 No discrete morphological characters distinguish the quadrate of *D. wilsoni* from those
394 of its closest relatives. As in other derived tyrannosaurines, the quadrate is massive, with a
395 shallow fossa on its medial surface and a pronounced pneumatic foramen (and surrounding
396 fossa) at the rostral confluence of the mandibular condyles and the orbital process (Fig. 9; Carr
397 et al., 2017). The paraquadrate foramen, bounded medially by the quadrate and laterally by the
398 quadratojugal, is small and teardrop-shaped; only its lateral margin is made up by the
399 quadratojugal, as the quadrate forms the dorsal and ventral borders of the foramen.

400 Although no palatal elements are known, the medial deflection of the quadrate's
401 pterygoid wing allows an approximation of the position of the pterygoids relative to the facial
402 skeleton, and suggests a broad orbitotemporal region, as in other tyrannosaurines.

403 *Dentary*

404 The dentary of *D. wilsoni* is deep, with a relatively straight ventral margin and a dorsal
405 (alveolar) margin that trends caudodorsally, increasing the depth of the mandible caudally (Fig.
406 10). As in other *Daspletosaurus*, the texturing of the dentary symphysis is more exaggerated in
407 *D. wilsoni* than non-*Daspletosaurus* tyrannosaurines (e.g., *Tyrannosaurus*, *Thanatotheristes*;
408 Voris et al., 2020), and is composed of several interlocking (presumably, as only the left dentary
409 is known) ridges and cusps. There are 17 dental alveoli, as in *D. horneri* (Carr et al., 2017), and a
410 sharp, narrow Meckelian groove with a rugose knob caudoventral to its rostral end. This knob is
411 present in both other species of *Daspletosaurus*, as well as *Tyrannosaurus*, *Tarbosaurus*, and
412 *Zhuchengtyrannus magnus*, but not *Thanatotheristes* or more basal tyrannosaurids (Carr et al.,
413 2017; Voris et al., 2020).

414 The lateral surface of the dentary of BDM 107 bears two intersecting grooves
415 caudoventral to the caudal termination of the alveolar margin (Fig. 10); the edges of these
416 grooves are beveled and are likely pathological. They may represent bite marks, as have been
417 described on the craniofacial bones of other tyrannosaurids (Voris et al., 2020; Brown, Currie,
418 and Therrien, 2021).

419 *Splénial*

420 The splénial of BDM 107 is typical of *Daspletosaurus* except in the size and form of the
421 mylohyoid foramen (Fig. 11). In most derived tyrannosaurines, including *D. torosus* and *D.*
422 *horneri*, this foramen is extremely large, roughly the same dorsoventral depth as the rostral
423 process of the splénial (Carr et al., 2017). In *D. wilsoni*, however, the foramen is dorsoventrally
424 shallow, and rostrocaudally elongate, such that it is ellipsoid in form and roughly half the
425 dorsoventral depth of the splénial's rostral process. This is most similar to the condition in
426 alioramins (Brusatte, Carr, and Norell, 2012) and *Appalachiosaurus* (Carr, Williamson, and
427 Schwimmer, 2005).

428 *Cervical vertebrae*

429 Four cervical vertebrae are preserved in BDM 107 from the cranial-middle portion of the
430 series. No atlas or axis were found. As in all tyrannosaurids, the spinous processes of the
431 cervical vertebrae are subequal in dorsoventral height to their corresponding centra. Both the
432 spinous processes and the centra are craniocaudally short, similar to and most exaggerated in
433 the cervical vertebrae of *Tyrannosaurus* (see Brochu, 2003, and figures therein). As in
434 *Tyrannosaurus* (and other large tyrannosaurids), the cranial and caudal faces of the cervical
435 centra are dorsoventrally displaced from one another in order to create the characteristic 'S-
436 curve' of the neck. The centrum of the third cervical vertebra in BDM 107 is extremely
437 foreshortened craniocaudally (i.e., much taller than long), indicating a robustly built cranial
438 portion of the neck, presumably in order to support the weight of the head.

439 *Sacral vertebrae*

440 The spinous processes of two sacral vertebrae are preserved. Both are sub-rectangular
441 in form and bear rugose knobs near their apices, presumably the ossified bases of sacral
442 ligaments.

443 **Methods**

444 The holotype specimen was collected under permit MTM 108829-e6 issued to DF by The
445 US Bureau of Land Management.

446 The electronic version of this article in Portable Document Format (PDF) will represent a
447 published work according to the International Commission on Zoological Nomenclature (ICZN),
448 and hence the new names contained in the electronic version are effectively published under
449 that Code from the electronic edition alone. This published work and the nomenclatural acts it
450 contains have been registered in ZooBank, the online registration system for the ICZN. The
451 ZooBank LSIDs (Life Science Identifiers) can be resolved and the associated information viewed
452 through any standard web browser by appending the LSID to the prefix <http://zoobank.org/>.
453 The LSID for this publication is: urn:lsid:zoobank.org:pub:F7EE2619-89FC-4D72-93DA-
454 EFE6BD549A77. The online version of this work is archived and available from the following
455 digital repositories: PeerJ, PubMed Central SCIE and CLOCKSS.

456 A cladistic phylogenetic analysis was conducted using the character matrix of Carr et al.
457 (2017) (with modifications from Voris et al., 2020), with additional modifications based on
458 personal observation of specimens made by the lead author, including the addition to the
459 character matrix of several proposed autapomorphies of *D. horneri* noted by Carr et al. (2017)
460 to occur more broadly across Tyrannosauridae (see Supplementary Information for a
461 comprehensive list of modifications). The analysis was run in TnT v1.5 (Goloboff, Farris, and
462 Nixon, 2008) using a “New Technology” search with settings identical to those of Voris et al.
463 (2020) (ratchet, tree drift, tree fusing, and sectorial search set to default, and set to recover
464 minimum length 10 times). Support for recovered clades was tested using bootstrapping with
465 1000 replicates under a traditional search.

466 **Results**

467 The cladistic analysis produced 12 Most Parsimonious Trees (MPTs; best score: 853).
468 Within the strict consensus of these trees, the least inclusive clade containing *Dynamoterror*
469 and *Tyrannosaurus* (i.e., all of Tyrannosaurinae more derived than *Alioramus*) was recovered as
470 a large polytomy, with a sister relationship retained between *Tyrannosaurus* and *Tarbosaurus*,
471 and *Dynamoterror*, *Lythronax*, and *Teratophoneus* recovered in a trichotomy (see
472 Supplementary Information: Fig. S1).

473 Given the fragmentary nature of their respective holotypes (scored for <15% of
474 characters), *Nanuqsaurus hoglundi* and *Thanatotheristes* were removed from the dataset
475 (inclusion of either taxon collapsed the tree as above), and an additional analysis was
476 conducted with the same settings. This analysis produced two MPTs (best score: 846), and
477 recovered *D. wilsoni* as sister to a clade formed by *D. horneri* and more derived tyrannosaurines
478 (*Zhuchengtyrannus*, *Tarbosaurus*, *Tyrannosaurus*). Alioramins were recovered within a

479 polytomy, as were *Dynamoterror*, *Teratophoneus*, and *Lythronax*; all other topological
480 relationships were as in Voris et al. (2020) (Fig. 12).

481 Bootstrapping of this result showed weak support (<70) for all clades within
482 Tyrannosaurinae except for alioramini (90), derived tyrannosaurines (*Daspletosaurus* +
483 (*Zhuchengtyrannus* (*Tyrannosaurus* + *Tarbosaurus*))) (82), tyrannosaurines more derived than
484 *Daspletosaurus* (85), and *Tyrannosaurus* + *Tarbosaurus* (85). Recovered support was particularly
485 weak (≤ 9) for the interrelationships of *Daspletosaurus* (Fig. 12).

486 A single autapomorphy of *D. wilsoni* was recovered by the cladistic analysis: mylohyoid
487 foramen of the splenial elongate and rostrocaudally ovoid (this foramen is much deeper in
488 other *Daspletosaurus* species; see above).

489 The *D. wilsoni* + more derived tyrannosaurines clade was recovered with the following
490 three synapomorphies: dorsoventrally tall orbit; mediolaterally oriented tooth row of the
491 premaxilla; and short cornual process of the lacrimal. A further four synapomorphies united *D.*
492 *horneri* and more derived tyrannosaurines to the exclusion of *D. wilsoni*: rostromedially directed
493 orbits (resulting from the rostromedial bowing of the jugal); cornual process of the postorbital
494 swollen and terminating far rostral to the laterotemporal fenestra; first interdental plate of the
495 maxilla narrow, and second plate truncated (both plates are subsequently expanded in
496 tyrannosaurines more derived than *D. horneri*); and mediolaterally oriented prefrontal.
497 Additional autapomorphies of relevant taxa and synapomorphies of relevant clades are
498 available in Supplementary Information.

499 Discussion

500 Several aspects of the results presented here contrast with (or supplement) those of
501 previous analyses, and therefore deserve mention. Noticeably, the results of the cladistic
502 analysis place *Tyrannosaurus* – line tyrannosaurines (*Zhuchengtyrannus*, *Tarbosaurus*, and
503 *Tyrannosaurus*) as successive sister taxa to *Daspletosaurus* (*contra* Carr et al., 2017, and Voris et
504 al., 2020, both of which recovered these as sister lineages), and recovers a paraphyletic
505 *Daspletosaurus*; these aspects of the results are the topic of a study by the lead author
506 currently in review, and will not be discussed here (although it should be noted that similar
507 results were recovered by Horner, Varricchio, and Goodwin, 1992, and the Bayesian analysis of
508 Brusatte and Carr, 2016; Loewen et al., 2013 also recovered a paraphyletic *Daspletosaurus*.
509 Should this paraphyly be upheld by future studies, *D. wilsoni* and *D. horneri* may be assigned
510 new genera in order to preserve monophyly; *D. wilsoni* is assigned to *Daspletosaurus* here to
511 avoid the creation of a polyphyletic *Daspletosaurus* and for ease of discussion and comparison
512 with its closest relatives). Instead, only the interrelationships and evolutionary history of
513 *Daspletosaurus* are considered below.

514 Though not included in the cladistic analysis, the Dinosaur Park taxon agrees with *D.*
515 *wilsoni* in several characters which differ in both of these taxa from the condition in *D. torosus*
516 (see Description), including the orientation of the premaxillary tooth row, the height of the
517 cornual process of the lacrimal, the inflation of the rostradorsal ala of the lacrimal, and lateral
518 exposure of the dorsal quadrate contact of the quadratojugal. All of these characters are also

519 shared with *D. horneri*, although *D. wilsoni* and the Dinosaur Park taxon also share (to the
520 exclusion of *D. horneri*) a cornual process of the postorbital that approaches the laterotemporal
521 fenestra and is subdivided into a caudodorsal tuberosity and a supraorbital shelf, and a
522 prefrontal that is oriented rostrocaudally rather than rostromedially or mediolaterally (both of
523 these characters are also present in *D. torosus*). Similarity in all of these features suggests a
524 close affinity between *D. wilsoni* and the Dinosaur Park taxon, although this could reflect either
525 taxonomic synonymy or a genuine sister relationship; this designation is reserved for future
526 studies centered on the Dinosaur Park taxon (noted as forthcoming by Currie, 2003 and
527 Carabajal et al., 2021), which has yet to receive a formal description and may reveal
528 autapomorphies (or synapomorphies with *D. wilsoni*) not considered here.

529 Should the Dinosaur Park taxon be demonstrated to represent a distinct species from *D.*
530 *wilsoni*, it would potentially represent the first known instance of contemporaneity between
531 more than one species of *Daspletosaurus* (Carr et al., 2017), given that the *D. wilsoni* holotype
532 was preserved in strata likely corresponding in time to the deposition of the Dinosaur Park
533 Formation (at least in part; see Geologic Context). However, this possibility rests both upon the
534 taxonomic distinctiveness of the Dinosaur Park taxon and the absence of fine-scale stratigraphic
535 separation between this species and *D. wilsoni*, both of which require additional study to
536 confirm or deny (e.g., a formal description of the anatomy of the Dinosaur Park taxon and
537 precise stratigraphic placement of individuals of this taxon and *D. wilsoni*). Discussion below will
538 therefore exclude this possibility from consideration, although resulting hypotheses will be
539 subject to revision should this exclusion prove to be erroneous.

540 Among described *Daspletosaurus* species, *D. wilsoni* fulfills the predictions made by Carr
541 et al.'s (2017) hypothesis of anagenesis between *D. torosus* and *D. horneri*. Namely, *D. wilsoni* is
542 stratigraphically, phylogenetically, and morphologically intermediate between these taxa (see
543 Geologic Context, Results, and Diagnosis, respectively), and occurs within the same general
544 geographic range (all three species of *Daspletosaurus* are found within Montana or Alberta;
545 Carr et al., 2017). These points correspond to the criteria proposed by Carr et al., 2017 (and
546 later Zietlow, 2020) for defensible hypotheses of anagenesis: (1) lack of stratigraphic overlap
547 (but see above), (2) close phylogenetic relationships, (3) intermediate morphologies, and (4)
548 similar geographic ranges. It should be noted that while the fulfillment of these criteria
549 establishes anagenesis as a defensible hypothesis, it does not preclude cladogenesis in
550 *Daspletosaurus* as the driving factor of the evolution of this genus (with successively more
551 derived clades, e.g., *D. wilsoni* and more derived tyrannosaurines, representing cladogenetic
552 events rather than portions of an anagenetic sequence).

553 However, several alternative lines of evidence are consistent with anagenesis and
554 inconsistent with cladogenesis, and therefore strengthen the hypothesis of anagenesis as a
555 predominant evolutionary mode in *Daspletosaurus*. Firstly, as noted by Wagner and Erwin
556 (1995), cladogenesis via punctuated equilibrium (with species diverging from an ancestral taxon
557 in morphological stasis; Eldredge and Gould, 1972) can be identified by the presence of
558 polytomies in a recovered cladogram, since descendant species of an ancestor in stasis will not
559 form subclades. No polytomy was recovered within the clade formed by *Daspletosaurus* and
560 more derived tyrannosaurines (Fig. 11); the origination of *Daspletosaurus* species by

561 punctuated equilibrium can therefore be rejected based on the topology of the recovered
562 cladogram alone. Secondly, *D. wilsoni* almost entirely **lacks autapomorphies**, displaying only a
563 single feature not also present in either *D. torosus* or *D. horneri* (a rostrocaudally elongate
564 mylohyoid foramen of the splenial, recovered by the cladistic analysis; see Results). Wagner and
565 Erwin (1995) and Szalay (1977) noted that ancestors should lack apomorphies relative to
566 descendants, such that a paucity of autapomorphies suggests that an ancestral taxon has been
567 sampled. Similarly, Wilson et al. (2020) noted the absence of autapomorphies in several
568 centrosaurine taxa hypothesized therein to represent an anagenetically evolving lineage, with
569 stratigraphically successive taxa being defined by combinations of plesiomorphic and
570 apomorphic characters rather than species-level autapomorphies (forming “metaspecies;”
571 Wilson et al., 2020; Horner, Varricchio, and Goodwin, 1992). Indeed, a hypothesis of
572 cladogenesis at the root of the clade formed by *D. wilsoni* and more derived tyrannosaurines
573 would rest **entirely upon** the elongate mylohyoid foramen of this species as evidence of
574 divergence from other *Daspletosaurus*; in the absence of additional characters supporting this
575 hypothesis, the sole autapomorphy of *D. wilsoni* may alternatively represent individual
576 variation, or a character evolved within this species and lost before the appearance of *D.*
577 *horneri* (similar to the lateral exposure of the dorsal quadrato contact of the quadratojugal,
578 present in *D. wilsoni* and the holotype of *D. horneri*, but not in the stratigraphically sequential
579 paratype specimen or more derived tyrannosaurines; see Description). The morphological
580 evidence for a cladogenetic origin of *D. wilsoni* is therefore weak; the blend of ancestral and
581 derived characteristics in this species and the near total absence of autapomorphies is more
582 consistent with anagenesis between stratigraphically antecedent (*D. torosus*) and subsequent
583 (*D. horneri*) taxa. In light of this evidence, we propose that the three species of this
584 *Daspletosaurus* represent an anagenetically evolving lineage (Fig. 13); as noted above, this
585 hypothesis will be subject to revision following further study into the phylogenetic affinities of
586 species within the genus, additional discoveries of *Daspletosaurus* individuals from
587 stratigraphically intermediate horizons (which under an anagenetic model, should be
588 intermediate in morphology between species), and characterization of the range of individual
589 variation present in relevant characters proposed here to represent species-level
590 autapomorphies or morphological transitions between taxa.

591 Should branching events (i.e., cladogenesis) within *Daspletosaurus* be demonstrated by
592 future studies or discoveries (e.g., if the Dinosaur Park taxon is demonstrated to be both
593 distinct from and contemporaneous with *D. wilsoni*), this would not necessarily exclude
594 anagenesis from playing a role in the generation of morphological novelty within the genus.
595 Wagner and Erwin (1995) noted the presence of anagenetic change between branching events
596 in plesiomorphic lineages (=ancestral lineages; the lineage from which cladogenetically derived
597 taxa branch) not in morphological stasis, which led these authors to designate this pattern of
598 speciation as “bifurcation,” reserving “cladogenesis” for branching from morphologically static
599 ancestral taxa. Although we do not adopt their terminology, we agree that anagenesis can
600 operate in concert with cladogenesis in order to produce observed patterns of
601 macroevolutionary change. In the case of *Daspletosaurus*, while autapomorphies of individual
602 species may represent the results of cladogenesis, the synapomorphies of progressively more
603 exclusive clades within the genus (e.g., coarse symphyseal texture of the dentary in

604 *Daspletosaurus*, inflated rostradorsal ala of the lacrimal in *D. wilsoni* + *D. horneri*, etc.) would
605 remain anagenetically derived under a typically cladogenetic model. Anagenesis therefore
606 enjoys a predominant role in the evolution of derived morphologies within derived
607 tyrannosaurines, regardless of the presence of branching events within *Daspletosaurus* (in
608 contrast to morphologically static genera, in which morphological change is concentrated at the
609 base of cladogenetic events; Eldredge and Gould, 1972).

610 The low bootstrap support recovered for the results of the cladistic analysis may also be
611 readily explained in the context of anagenesis. As noted by Soltis and Soltis (2003), low
612 bootstrap scores may be recovered for otherwise well-supported clades (e.g., clades recovered
613 within all MPTs, as in all of the interrelationships of *Daspletosaurus* recovered here) if they are
614 supported by few characters, given that the chance of supporting characters being included in a
615 bootstrap resample is lower with fewer characters. This is a common occurrence among
616 recently diverged clades which have not had much time to accrue synapomorphies (Soltis and
617 Soltis, 2003), but the same would apply to an anagenetically evolving *Daspletosaurus*; should *D.*
618 *wilsoni* represent a descendant of *D. torosus* as proposed here, then all of the synapomorphies
619 of the *D. wilsoni* + more derived tyrannosaurines clade must have been evolved within the ~500
620 Ka window between *D. torosus* and *D. wilsoni* (it should be noted that this would also be true in
621 the case of recent divergence of the *D. wilsoni* + more derived tyrannosaurine clade via
622 cladogenesis; therefore, low bootstrap scores cannot be taken as evidence of anagenesis, but
623 are at least consistent with it).

624 More generally, as sampling of a lineage increases, the temporal windows between
625 sampled taxa must necessarily be reduced, and synapomorphies of progressively more derived
626 clades will therefore be fewer (with the same number of character changes distributed among
627 more clades as sampling increases), such that bootstrap scores can be expected to correlate
628 negatively with sampling intensity. To this point, removal of *D. wilsoni* (in addition to
629 *Nanuqsaurus* and *Thanatotheristes*, as described above; see Results) from the cladistic analysis
630 recovers an identical tree topology, but increases bootstrap support for the *D. horneri* + more
631 derived tyrannosaurines clade from 8 to 25 (still a low score, **to be sure**, but over three times
632 higher).

633 Bootstrap scores can also be affected by the inclusion of characters irrelevant to the
634 node in question (Soltis and Soltis, 2003). The phylogenetic character matrix of Carr et al. (2017)
635 used here contains characters informative across Tyrannosauroidae, including hundreds of
636 characters that are not informative within *Daspletosaurus* or derived Tyrannosaurinae in
637 general (i.e., characters not recovered as autapomorphies or synapomorphies for species or
638 groups within this clade, respectively). We therefore regard the low bootstrap scores recovered
639 for the phylogenetic placement of *D. wilsoni* not as evidence of an erroneous result, but as an
640 expected consequence of higher taxonomic resolution among derived tyrannosaurines and the
641 nature of the data matrix used.

642 **Conclusions**

643 *D. wilsoni* sp. nov., a stratigraphic and morphological intermediate between *D. torosus*
644 and *D. horneri*, is hypothesized to represent a transitional form along an anagenetic lineage
645 linking both previously named species of *Daspletosaurus*. This finding, in concert with previous
646 identifications of anagenesis in contemporary dinosaur lineages, emphasizes the explanatory
647 power of anagenesis in the production of evolutionary trends among dinosaurs of the Late
648 Cretaceous Western Interior (Scannella et al., 2014; Freedman Fowler and Horner; Fowler and
649 Freedman Fowler, 2020; **Wilson et al., 2020**). Indeed, as anagenesis continues to be identified
650 among fossil lineages, the predominant relative frequency of strictly cladogenetic evolutionary
651 models (e.g., punctuated equilibria; Eldredge and Gould, 1972) must eventually come under
652 scrutiny. Future explorations of evolutionary mode in fossil taxa, including further tests of the
653 hypotheses presented here, will be important in this regard, and have the potential to refine
654 understanding of the pattern and process of dinosaur evolution.

655 **Institutional Abbreviations**

656 AMNH – American Museum of Natural History, New York, New York, USA

657 BDM – Badlands Dinosaur Museum, Dickinson Museum Center, Dickinson, North Dakota, USA

658 CMN – Canadian Museum of Nature, Ottawa, Ontario, Canada

659 FMNH – Field Museum of Natural History, Chicago, Illinois, USA

660 GIN – Palaeontological Centre of the Mongolian Academy of Sciences, Ulaanbaatar, Mongolia

661 GM – Ganzhou Museum, Ganzhou, China

662 MOR – Museum of the Rockies, Bozeman, Montana, USA

663 TMP – Royal Tyrrell Museum of Paleontology, Drumheller, Alberta, Canada

664 UALVP – University of Alberta Laboratory for Vertebrate Palaeontology, Edmonton, Alberta,
665 Canada

666 UMNH – Natural History Museum of Utah, Salt Lake City, Utah, USA

667 ZPAL – Institute of Palaeobiology of the Polish Academy of Sciences, Warsaw, Poland

668 **Acknowledgments**

669 Special thanks are given to John Wilson for his discovery of the holotype specimen.
670 Thanks also to Elizabeth Freedman Fowler and Matthew Lavin for discussion and guidance that
671 improved the quality of this manuscript, and to David Hone, Jared Voris, and Thomas Holtz for
672 helpful reviews. Thanks to Joshua Chase, Greg Liggett, Pat Gunderson, and other employees of
673 the Bureau of Land Management who assisted DF with land access, permitting, and excavation.
674 We would also like to thank the members of BDM field crews that worked tirelessly to excavate
675 “Jack’s B2,” including Meara Aberle, Jon Carr, Andrew Chappelle, Steven Clawson, Chalfant
676 Conley, Brian Conway, Joshua deOlivera, Jordan Drost, Robert Ebelhar, Elizabeth Flint, Elizabeth
677 Freedman Fowler, Joshua Fry, Sandi Guarino, Brad Hoole, Felipe Jannarone, Marianna
678 Karagiannis, Ashley Lambert, Rachel Livengood, Kat Maguire, Marianna Rogers, Emily Waldman,

679 Solin Wanders, Alyssa Wieggers, Jack Wilson, and many others, without whom study of the
680 holotype specimen would not have been possible. Thanks to Steven Clawson, Amanda Hendrix,
681 Destiny Wolf, and Darrah Steffen for their preparation and curation of the holotype specimen.
682 Thanks also to the Bergtohl family for land access, and to Matt Poole and Montana State Office
683 Glasgow for camping access.

684 **References**

- 685 1. Brochu, C. A. (2003). Osteology of **Tyrannosaurus rex**: insights from a nearly complete
686 skeleton and high-resolution computed tomographic analysis of the skull. *Journal of*
687 *Vertebrate Paleontology*, 22(sup4), 1-138.
- 688 2. Brown, C. M., Currie, P. J., & Therrien, F. (2022). Intraspecific facial bite marks in
689 tyrannosaurids provide insight into sexual maturity and evolution of bird-like intersexual
690 display. *Paleobiology*, 48(1), 12-43.
- 691 3. Brusatte, S. L., Carr, T. D., & Norell, M. A. (2012). The osteology of *Alioramus*, a gracile
692 and long-snouted tyrannosaurid (Dinosauria: Theropoda) from the Late Cretaceous of
693 Mongolia. *Bulletin of the American Museum of Natural History*, 2012(366), 1-197.
- 694 4. Brusatte, S. L., & Carr, T. D. (2016). The phylogeny and evolutionary history of
695 tyrannosauroid dinosaurs. *Scientific Reports*, 6(1), 1-8.
- 696 5. Brusatte, S. L., Norell, M. A., Carr, T. D., Erickson, G. M., Hutchinson, J. R., Balanoff, A.
697 M., ... & Xu, X. (2010). Tyrannosaur paleobiology: new research on ancient exemplar
698 organisms. *science*, 329(5998), 1481-1485.
- 699 6. Brusatte, S. L., Sakamoto, M., Montanari, S., & Harcourt Smith, W. E. H. (2012). The
700 evolution of cranial form and function in theropod dinosaurs: insights from geometric
701 morphometrics. *Journal of Evolutionary Biology*, 25(2), 365-377.
- 702 7. Carpenter, K. (1990). Variation in *Tyrannosaurus rex*. *Dinosaur systematics: perspectives*
703 *and approaches*, 141-145.
- 704 8. Carr, T. D. (1999). Craniofacial ontogeny in tyrannosauridae (Dinosauria,
705 Coelurosauria). *Journal of vertebrate Paleontology*, 19(3), 497-520.
- 706 9. Carr, T. D. (2020). A high-resolution growth series of *Tyrannosaurus rex* obtained from
707 multiple lines of evidence. PeerJ 8:e9192, DOI 10.7717/peerj.9192
- 708 10. Carr, T. D., & Williamson, T. E. (2004). Diversity of late Maastrichtian Tyrannosauridae
709 (Dinosauria: Theropoda) from western North America. *Zoological Journal of the Linnean*
710 *Society*, 142(4), 479-523.
- 711 11. Carr, T. D., Varricchio, D. J., Sedlmayr, J. C., Roberts, E. M., & Moore, J. R. (2017). A new
712 tyrannosaur with evidence for anagenesis and crocodile-like facial sensory
713 system. *Scientific Reports*, 7(1), 1-11.
- 714 12. Carr, T. D., Williamson, T. E., & Schwimmer, D. R. (2005). A new genus and species of
715 tyrannosauroid from the Late Cretaceous (Middle Campanian) Demopolis Formation of
716 Alabama. *Journal of vertebrate Paleontology*, 25(1), 119-143.
- 717 13. Carr, T. D., Williamson, T. E., Britt, B. B., & Stadtman, K. (2011). Evidence for high
718 taxonomic and morphologic tyrannosauroid diversity in the Late Cretaceous (Late
719 Campanian) of the American Southwest and a new short-skulled tyrannosaurid from the
720 Kaiparowits formation of Utah. *Naturwissenschaften*, 98(3), 241-246.

- 721 14. Carr, T., Varricchio, D., Sedlmayr, J. *et al* (2017). A new tyrannosaur with evidence for
722 anagenesis and crocodile-like facial sensory system. *Sci Rep* 7, 44942.
- 723 15. Currie, P. J. (2003). Cranial anatomy of tyrannosaurid dinosaurs from the Late
724 Cretaceous of Alberta, Canada. *Acta Palaeontologica Polonica* 48 (2): 191–226.
- 725 16. Eberth, D. A., Currie, P. J., & Koppelhus, E. B. (2005). 3. *The Geology* (pp. 54-82).
726 Bloomington: Indiana University Press.
- 727 17. Goloboff, P. A., Farris, J. S., & Nixon, K. C. (2008). TNT, a free program for phylogenetic
728 analysis. *Cladistics*, 24(5), 774-786.
- 729 18. Gould, S. J., & Eldredge, N. (1972). Punctuated equilibria: an alternative to phyletic
730 gradualism. *Models in paleobiology*, 1972, 82-115.
- 731 19. Fiorillo, A. R., & Tykoski, R. S. (2014). A diminutive new tyrannosaur from the top of the
732 world. *PLoS One*, 9(3), e91287.
- 733 20. Foster, W., Brusatte, S. L., Carr, T. D., Williamson, T. E., Yi, L., & Lü, J. (2021). The cranial
734 anatomy of the long-snouted tyrannosaurid dinosaur *Qianzhousaurus sinensis* from the
735 Upper Cretaceous of China. *Journal of Vertebrate Paleontology*, 41(4), e1999251.
- 736 21. Foth C, Hedrick BP, Ezcurra MD (2016). Cranial ontogenetic variation in early saurischians
737 and the role of heterochrony in the diversification of predatory dinosaurs. *PeerJ* 4:e1589
- 738 22. Foth, C and Rauhut, O. W. M. (2013a). The Good, the Bad, and the Ugly: The Influence of
739 Skull Reconstructions and Intraspecific Variability in Studies of Cranial Morphometrics in
740 Theropods and Basal Saurischians. *PLoS ONE* 8(8): e72007.
- 741 23. Foth, C and Rauhut, O. W. M. Rauhut (2013b). Macroevolutionary and
742 Morphofunctional Patterns in Theropod Skulls: A Morphometric Approach. *Acta*
743 *Palaeontologica Polonica* 58(1), 1-6.
- 744 24. Fowler DW (2017) Revised geochronology, correlation, and dinosaur stratigraphic
745 ranges of the Santonian-Maastrichtian (Late Cretaceous) formations of the Western
746 Interior of North America. *PLoS ONE* 12(11): e0188426.
- 747 25. Fowler, D. W., & Fowler, E. A. F. (2020). Transitional evolutionary forms in
748 chasmosaurine ceratopsid dinosaurs: evidence from the Campanian of New
749 Mexico. *PeerJ*, 8, e9251.
- 750 26. Freedman Fowler, E. A., & Horner, J. R. (2015). A new brachylophosaurin hadrosaur
751 (Dinosauria: Ornithischia) with an intermediate nasal crest from the Campanian Judith
752 River Formation of northcentral Montana. *PloS one*, 10(11), e0141304.
- 753 27. Gignac, P. M., & Erickson, G. M. (2017). The biomechanics behind extreme osteophagy
754 in *Tyrannosaurus rex*. *Scientific Reports*, 7(1), 1-10.
- 755 28. Horner, J. R., Varricchio, D. J., & Goodwin, M. B. (1992). Marine transgressions and the
756 evolution of Cretaceous dinosaurs. *Nature*, 358(6381), 59-61.
- 757 29. Hurum, J.H. and Sabath, K. (2003). Giant theropod dinosaurs from Asia and North
758 America: Skulls of *Tarbosaurus bataar* and *Tyrannosaurus rex* compared. *Acta*
759 *Palaeontologica Polonica* 48 (2): 161–190.
- 760 30. Loewen, M. A., Irmis, R. B., Sertich, J. J., Currie, P. J., & Sampson, S. D. (2013). Tyrant
761 dinosaur evolution tracks the rise and fall of Late Cretaceous oceans. *PloS one*, 8(11),
762 e79420.
- 763 31. Lü, J., Yi, L., Brusatte, S. L., Yang, L., Li, H., & Chen, L. (2014). A new clade of Asian Late
764 Cretaceous long-snouted tyrannosaurids. *Nature communications*, 5(1), 1-10.

- 765 32. Matthew, W. D. and Brown, B. (1922). The family Deinodontidae, with notice of a new
766 genus from the Cretaceous of Alberta. *Bulletin of the American Museum of Natural*
767 *History* 46(6):367-385
- 768 33. Matthew, W. D., & Brown, B. (1923). Preliminary notices of skeletons and skulls of
769 Deinodontidae from the Cretaceous of Alberta. *American Museum novitates*; no. 89.
- 770 34. McDonald, A. T., Wolfe, D. G., & Dooley Jr, A. C. (2018). A new tyrannosaurid
771 (Dinosauria: Theropoda) from the Upper Cretaceous Menefee Formation of New
772 Mexico. *PeerJ*, 6, e5749.
- 773 35. Ogg JG, Hinnov LA. Cretaceous. In: Gradstein FM, Ogg JG, Schmitz MD, Ogg G, editors.
774 *The Geologic Time Scale*. 2. Oxford, UK: Elsevier; 2012. p. 793–853.
- 775 36. Osborn, H. F. (1905). Article XIV.-*Tyrannosaurus* and other Cretaceous dinosaurs. *Proc.*
776 *Acad. Nat. Sci. Phila*, 8, 72.
- 777 37. Osborn, H. F. (1912). Crania of *Tyrannosaurus* and *Allosaurus*; Integument of the
778 iguanodont dinosaur *Trachodon*. *Memoirs of the AMNH*; new ser., v. 1, pt. 1-2.
- 779 38. Paulina Carabajal, A., Currie, P. J., Dudgeon, T. W., Larsson, H. C., & Miyashita, T. (2021).
780 Two braincases of Daspletosaurus (Theropoda: Tyrannosauridae): anatomy and
781 comparison1. *Canadian Journal of Earth Sciences*, 58(9), 885-910.
- 782 39. Rogers, R. R., Kidwell, S. M., Deino, A. L., Mitchell, J. P., Nelson, K., & Thole, J. T. (2016).
783 Age, correlation, and lithostratigraphic revision of the Upper Cretaceous (Campanian)
784 Judith River Formation in its type area (north-central Montana), with a comparison of
785 low-and high-accommodation alluvial records. *The Journal of Geology*, 124(1), 99-135.
- 786 40. Russell, D. A. (1970). Tyrannosaurs from the Late Cretaceous of western Canada.
787 Ottawa: National Museum of Natural Sciences, Publications in Palaeontology, No. 1.
- 788 41. Scannella, J. B., Fowler, D. W., Goodwin, M. B., & Horner, J. R. (2014). Evolutionary
789 trends in Triceratops from the Hell Creek formation, Montana. *Proceedings of the*
790 *National Academy of Sciences*, 111(28), 10245-10250.
- 791 42. Sereno, P. C., McAllister, S., & Brusatte, S. L. (2005). TaxonSearch: a relational database
792 for suprageneric taxa and phylogenetic definitions. *Phyloinformatics*, 8(56), 1-25.
- 793 43. Soltis, P. S., & Soltis, D. E. (2003). Applying the bootstrap in phylogeny
794 reconstruction. *Statistical Science*, 256-267.
- 795 44. Szalay, F. S. (1977). Ancestors, descendants, sister groups and testing of phylogenetic
796 hypotheses. *Systematic Biology*, 26(1), 12-18.
- 797 45. Tanke, D.H. and Currie, P.J. (2010). A history of *Albertosaurus* discoveries in Alberta,
798 Canada. *Canadian Journal of Earth Sciences*. 47(9): 1197 -1211.
- 799 46. Voris, J. T., Therrien, F., Zelenitsky, D. K., & Brown, C. M. (2020). A new tyrannosaurine
800 (Theropoda: Tyrannosauridae) from the Campanian Foremost Formation of Alberta,
801 Canada, provides insight into the evolution and biogeography of
802 tyrannosaurids. *Cretaceous Research*, 110, 104388.
- 803 47. Wagner, P. J., Erwin, D. H., & Anstey, R. L. (1995). Phylogenetic patterns as tests of
804 speciation models. *New approaches to speciation in the fossil record*. *Columbia*
805 *University Press, New York*, 87-122.
- 806 48. Warshaw, E. A. (In Review). A reevaluation of evolutionary mode in derived
807 tyrannosaurines. *PeerJ*.

- 808 49. Wilson, J. P., Ryan, M. J., & Evans, D. C. (2020). A new, transitional centrosaurine
809 ceratopsid from the Upper Cretaceous Two Medicine Formation of Montana and the
810 evolution of the 'Styracosaurus-line' dinosaurs. *Royal Society Open Science*, 7(4),
811 200284.
- 812 50. Zietlow, A. R. (2020). Craniofacial ontogeny in Tylosaurinae. *PeerJ*, 8, e10145.

813

Figure 1

Map of the area of discovery of BDM 107, holotype of *D. wilsoni* sp. nov.

Nearby towns (Hinsdale, Glasgow, Saco) and highways (US-2) are labeled. Dashed lines indicate county boundaries; "Jack's B2" site indicated by star.

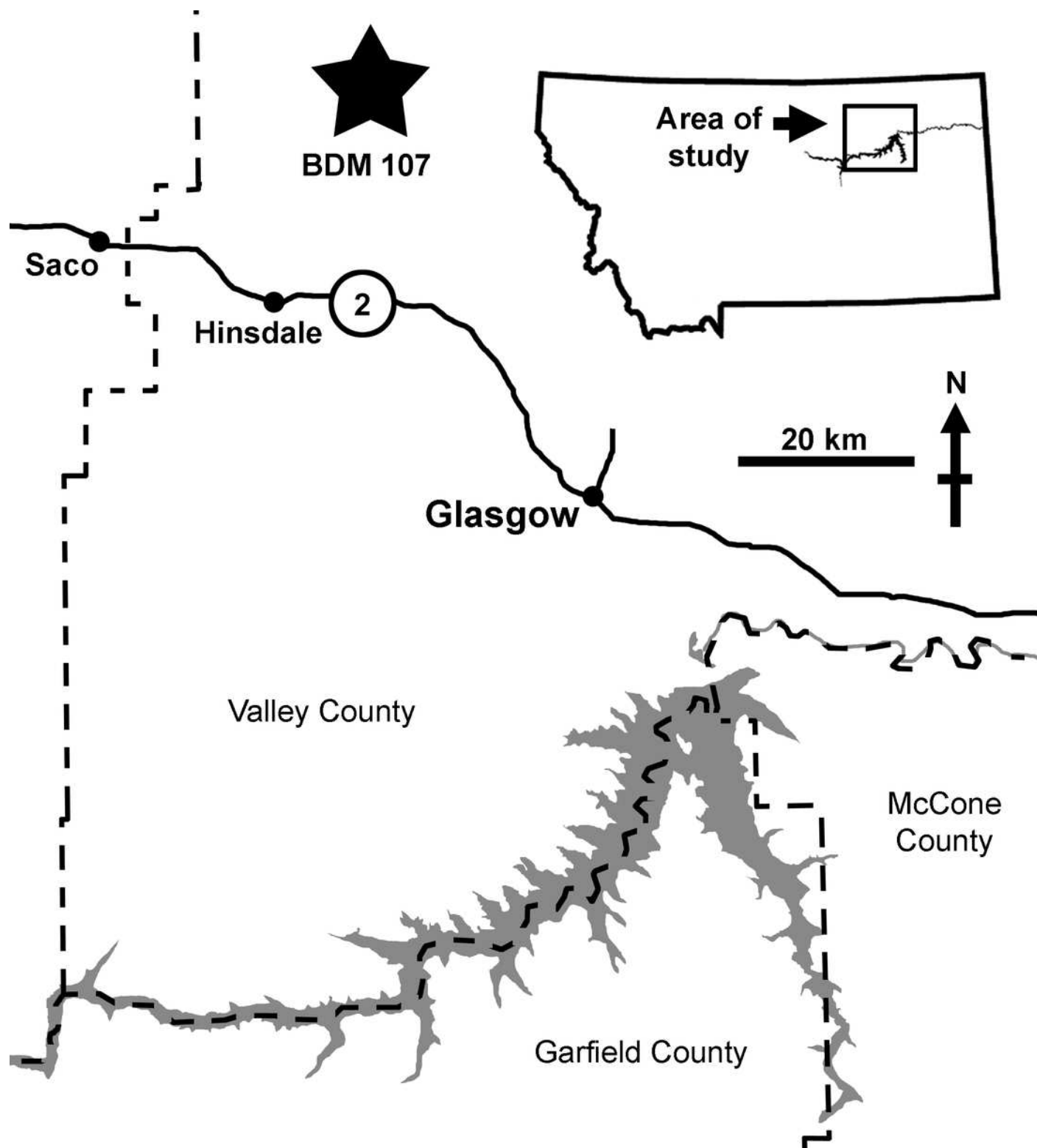


Figure 2

Premaxillae of BDM 107.

Shown in lateral (A), medial (B), and rostral (C) views. Abbreviations are as follows: nf, neurovascular foramina; smp, symphysis. Scale is 10 cm.

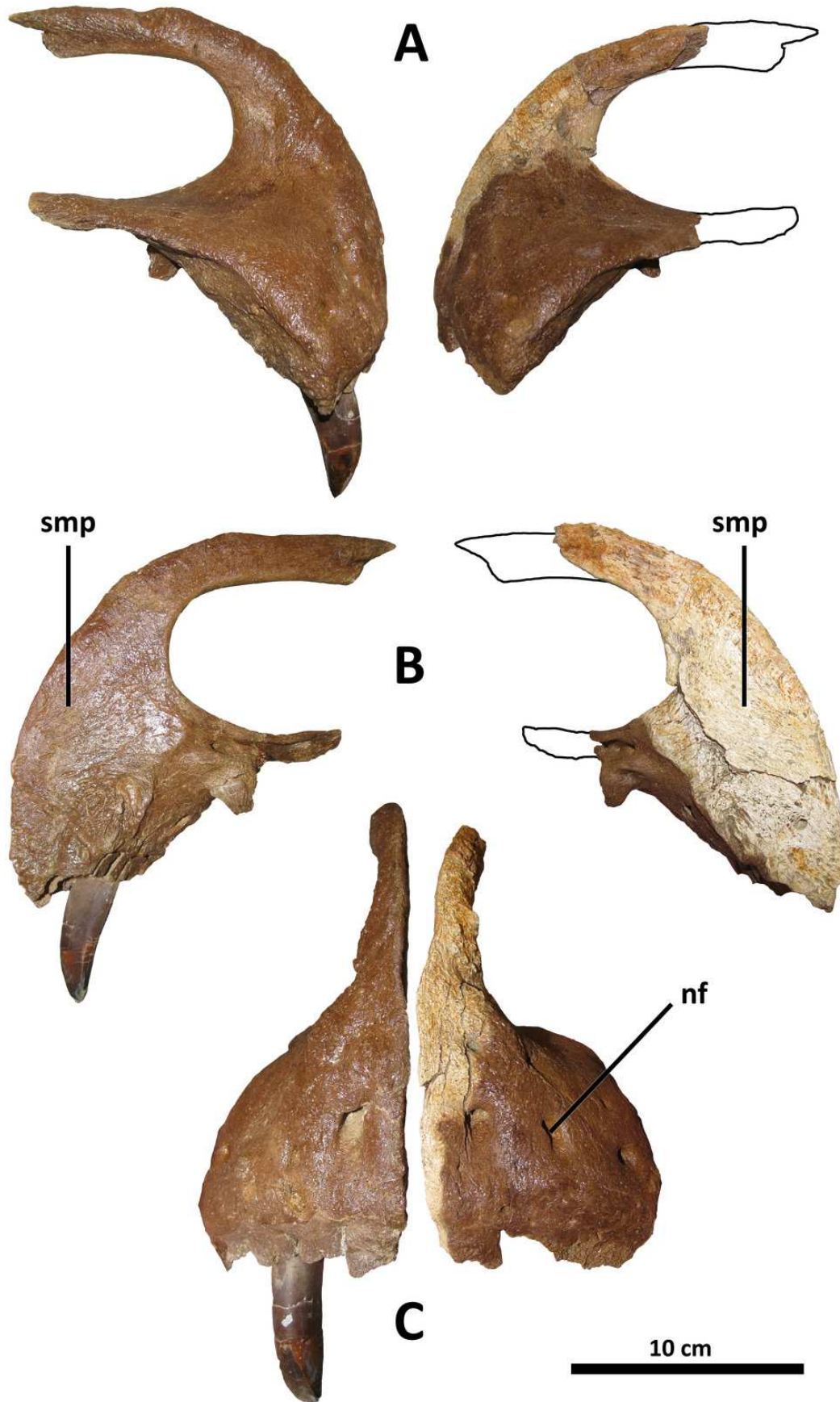


Figure 3

Left maxilla of BDM 107.

Shown in lateral (A) and medial (B) views. Abbreviations are as follows: af, antorbital fossa; aof, antorbital fenestra; ma, maxillary antrum; mxf, maxillary fenestra; pmr, promaxillary recess; pmx, promaxillary fenestra; ps, palatal shelf; nf, neurovascular foramina; ns, neurovascular sulci. Scale is 10 cm.

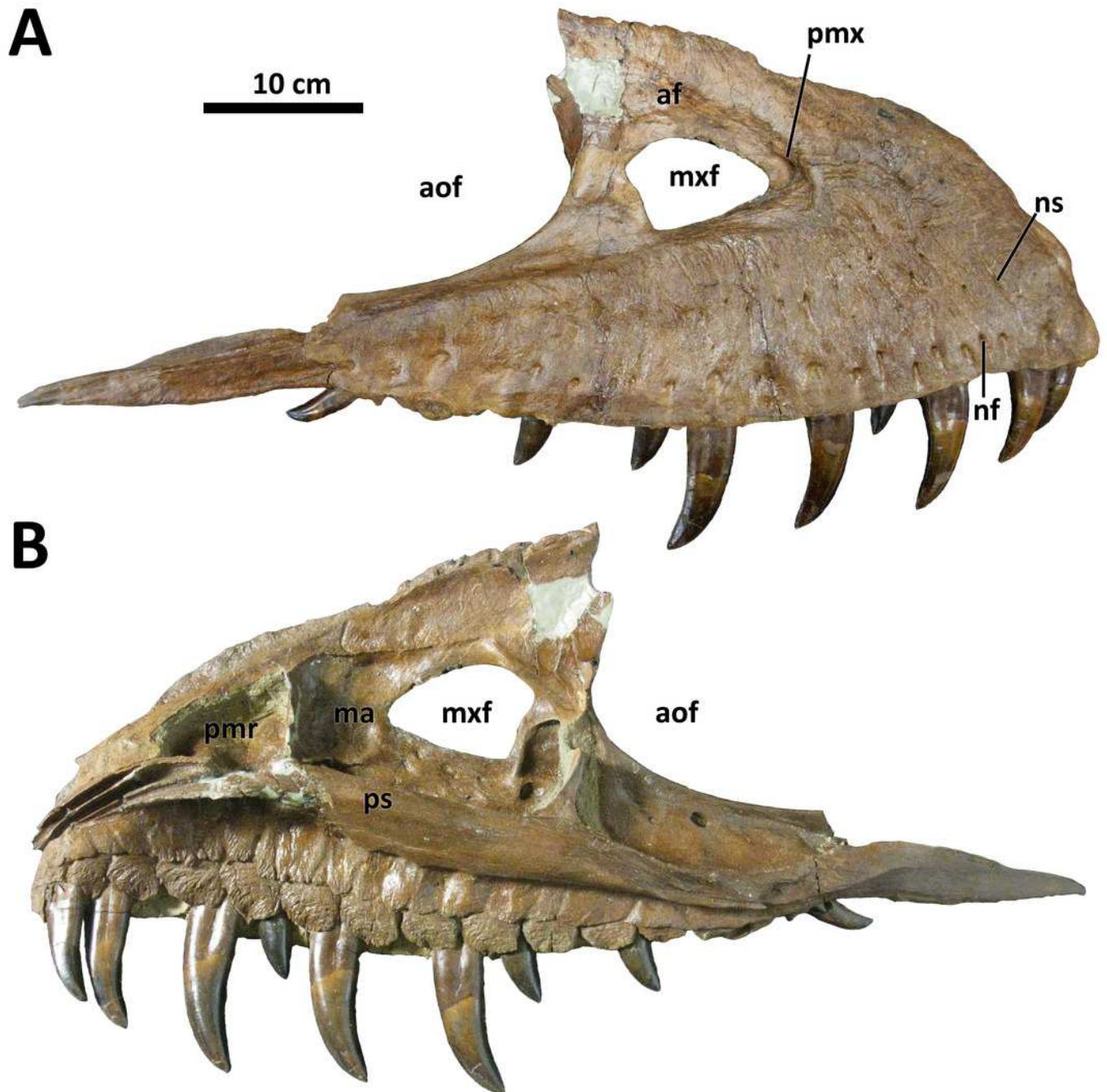


Figure 4

Right jugal of BDM 107.

Shown in medial (A) and lateral (B) views. Abbreviations are as follows: cp, cornual process; po, pneumatic opening; pop, postorbital process. Scale is 10 cm.

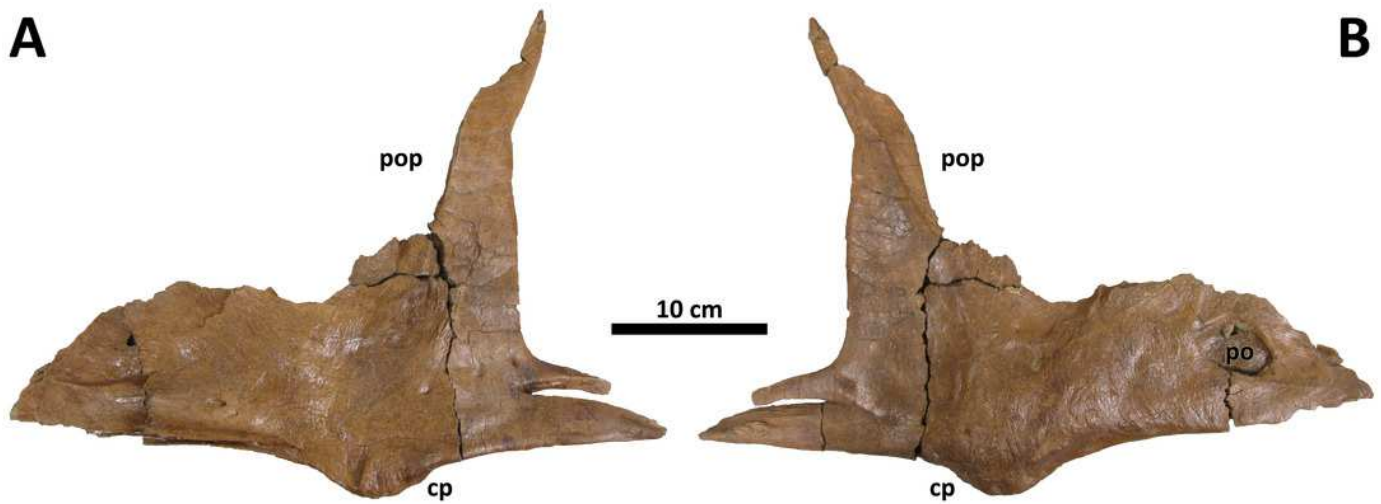


Figure 5

Left lacrimal of BDM 107.

Shown in lateral (A), medial (B), and dorsal (C) views. Abbreviations are as follows: cpa, cornual process apex; fr, frontal ramus; po, pneumatic opening; rda, rostradorsal ala; rr, rostral ramus; vp, ventral process; vr, ventral ramus. Scale is 10 cm.

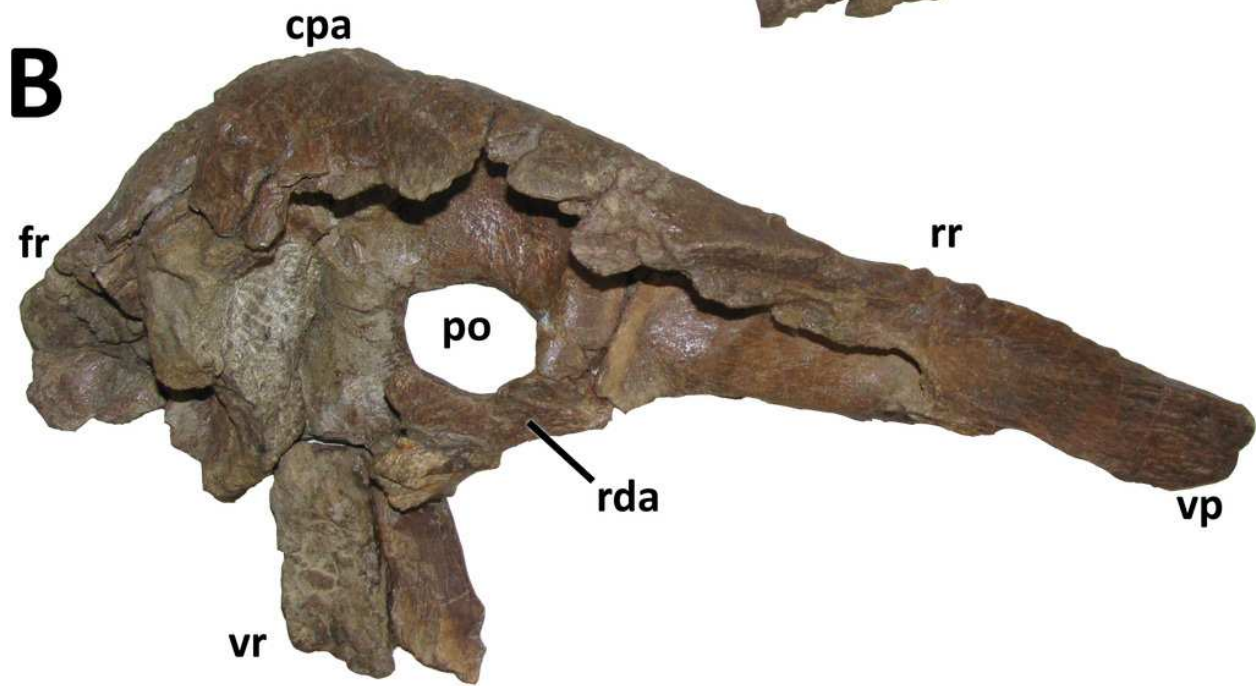
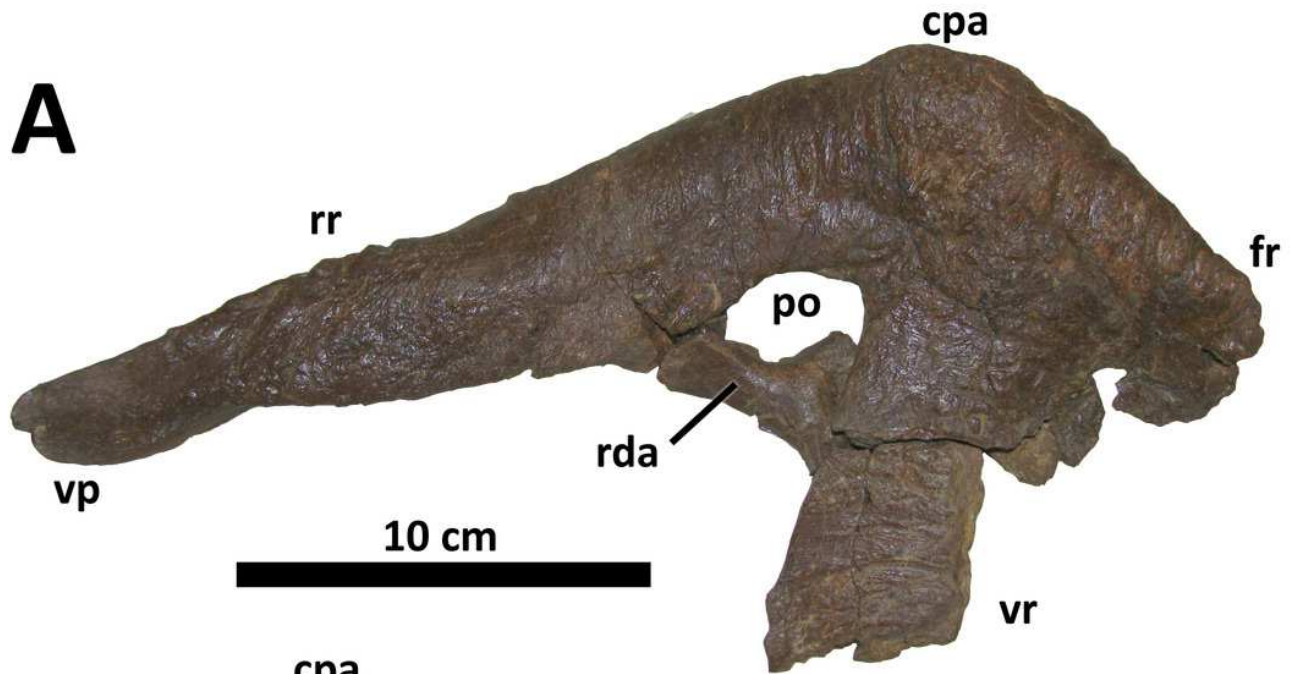


Figure 6

Left postorbital of BDM 107.

Shown in lateral (A), dorsal (B), medial (C), caudal (D), and rostral (E) views. Abbreviations are as follows: cdt, caudodorsal tuberosity; dtf, dorsotemporal fossa; fc, frontal contact; lsc, laterosphenoid contact; sop, subocular process; sos, supraorbital shelf. Scale is 10 cm.

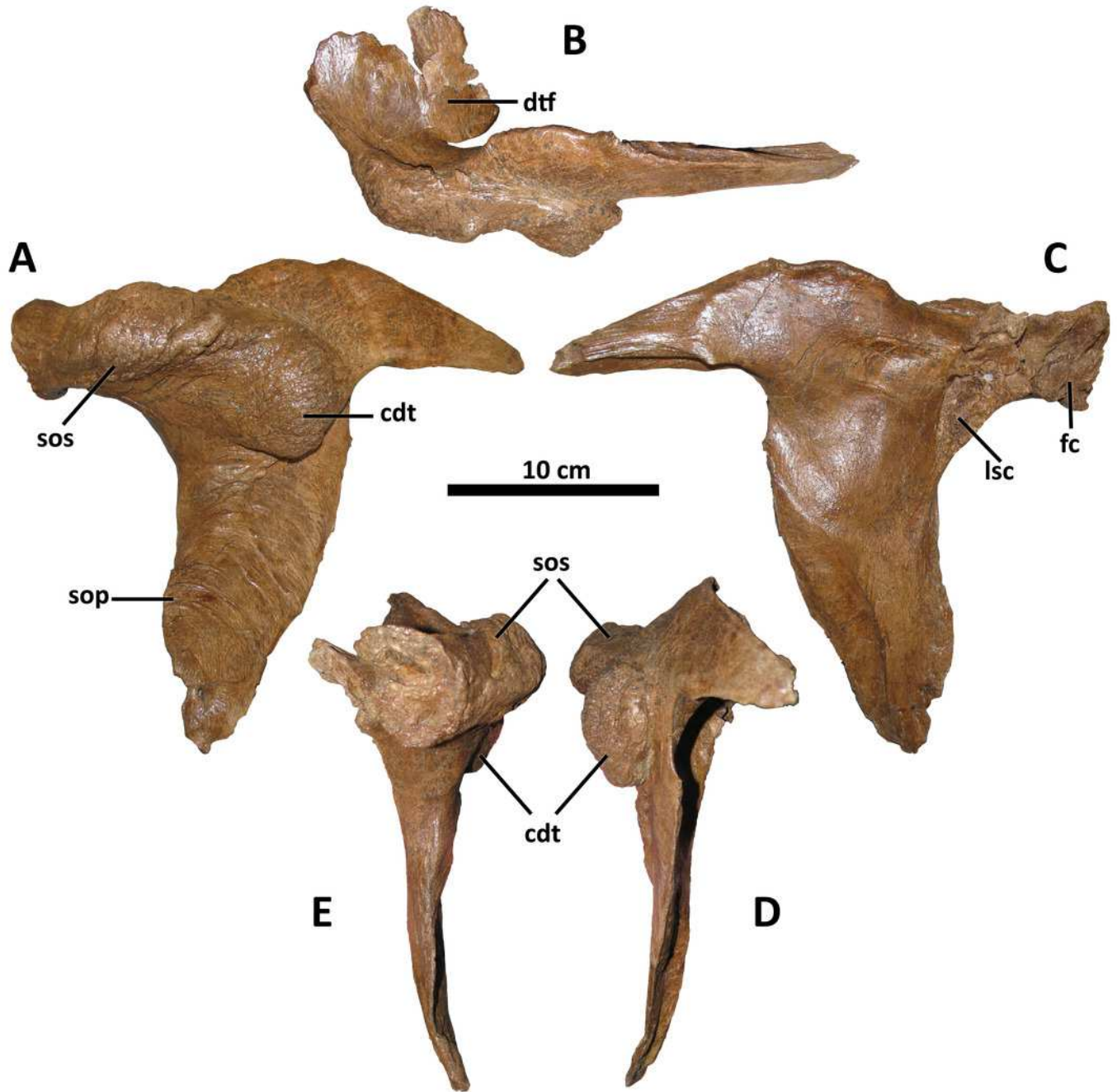


Figure 7

Left squamosal of BDM 107.

Shown in lateral (A), medial (B), and rostral (C) views. Abbreviations are as follows: cp, caudal process; ltf, laterotemporal fenestra; pcs, postorbital contact surface; po, pneumatic opening, qjp, quadratojugal process; rmm, rostromedial margin of pneumatic recess. Scale is 10 cm.

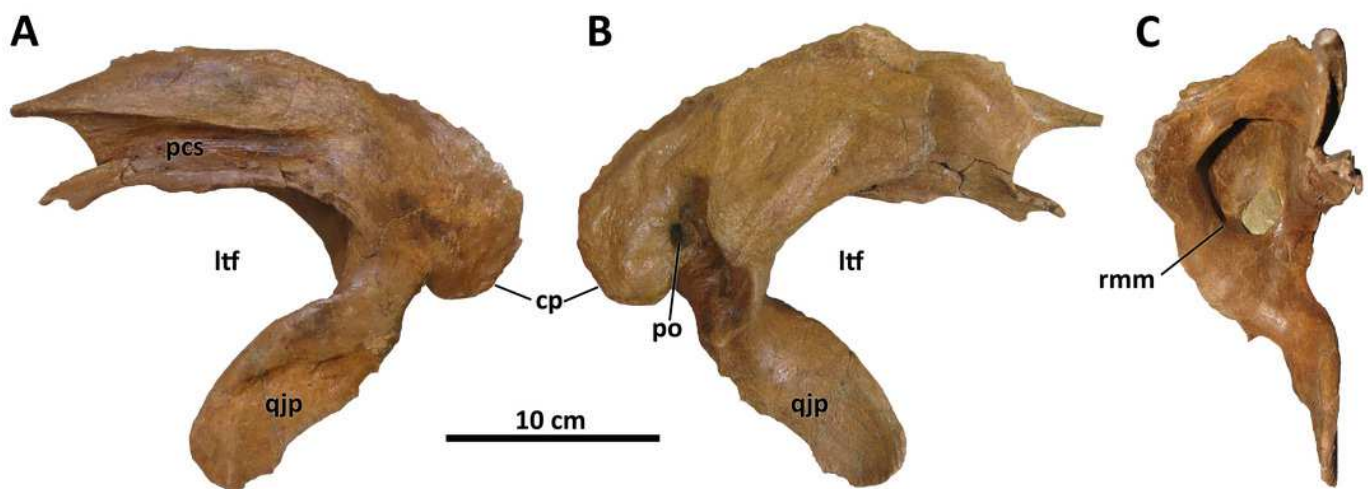


Figure 8

Right quadratojugal of BDM 107.

Shown in lateral (A) and medial (B) views. Abbreviations are as follows: dqc, dorsal quadrate contact; jr, jugal ramus; sc, squamosal contact; vqc, ventral quadrate contact. Scale is 10 cm.

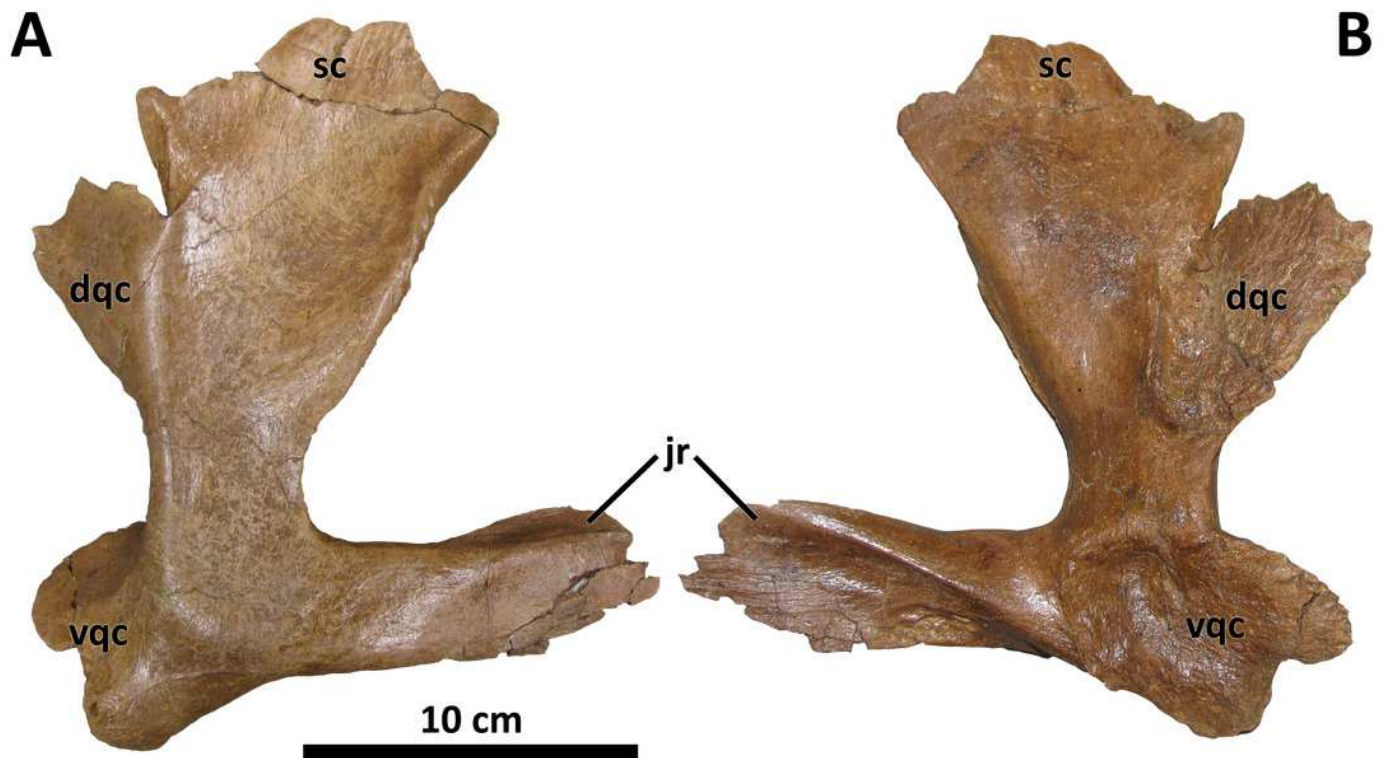


Figure 9

Right quadrate of BDM 107.

Shown in medial (A) and lateral (B) views. Abbreviations are as follows: op, orbital process; mc, mandibular condyles; po, pneumatic opening; pqf, paraquadrate foramen. Scale is 10 cm.

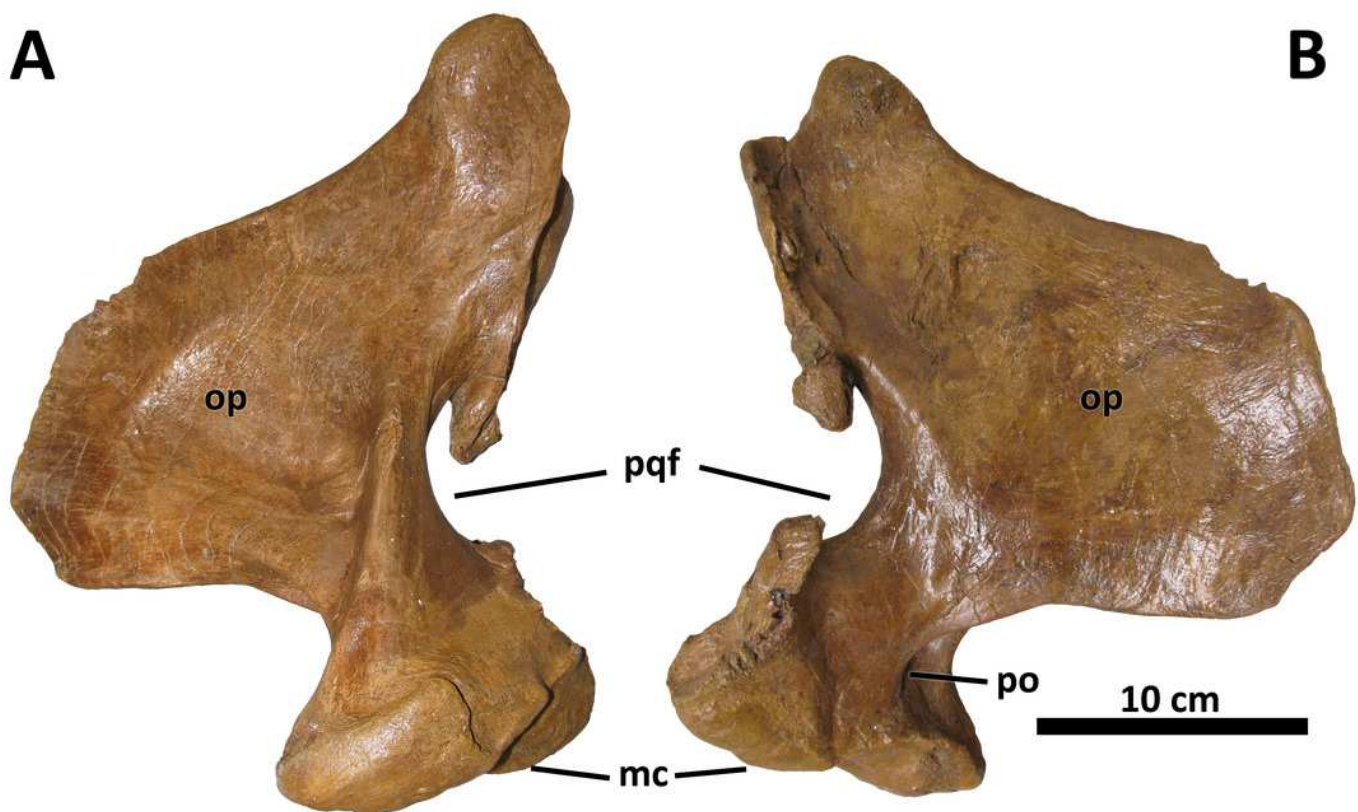


Figure 10

Right dentary of BDM 107.

Shown in lateral (A) and medial (B) views. Abbreviations are as follows: dc, dentary chin; dg, dentary groove; mcf, Meckelian foramen; mg, Meckelian groove; nf, neurovascular foramina; ns, neurovascular sulci; pt, pathology. Scale is 10 cm.

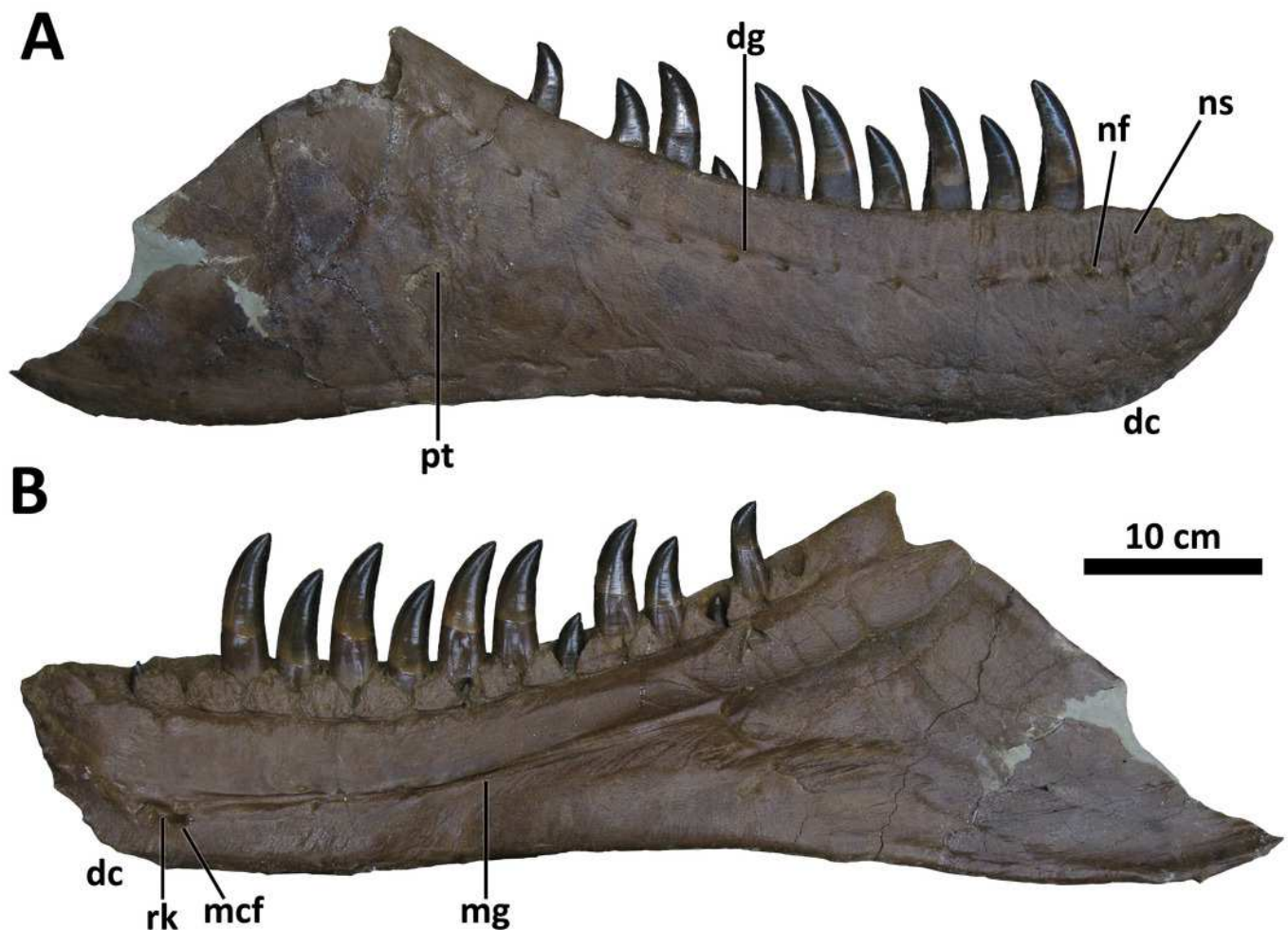


Figure 11

Right splenial of BDM 107.

Shown in medial (A) and lateral (B) views. Abbreviations are as follows: dcs, dentary contact surface; mhf, mylohyoid foramen. Scale is 10 cm.

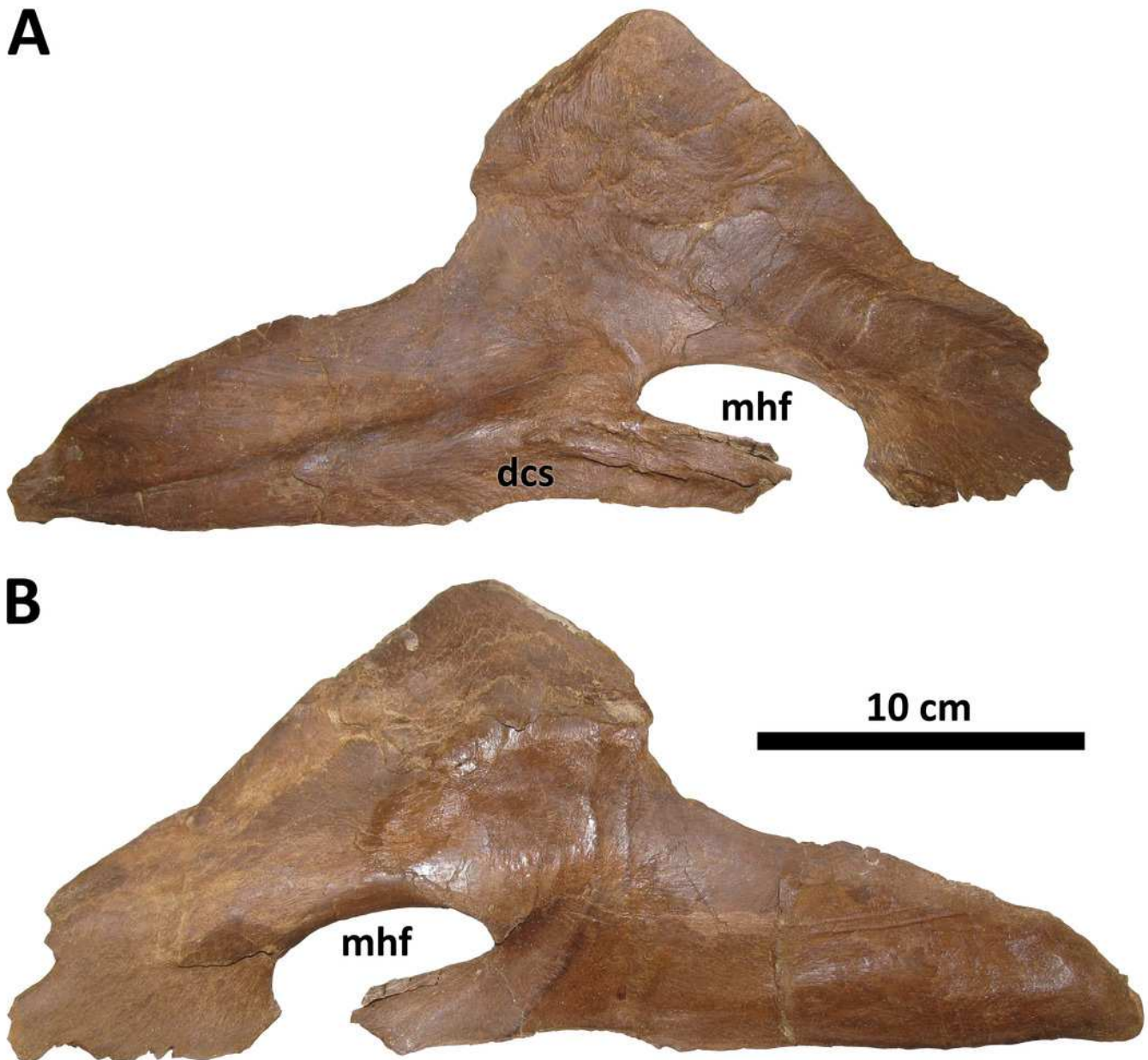


Figure 12

Results of the cladistic analysis.

Grey nodes denote *Daspletosaurus*, star denotes *D. wilsoni*, and numbers by each node are bootstrap support. Skull reconstruction represents the holotype of *D. wilsoni*, BDM 107 (known material in white).

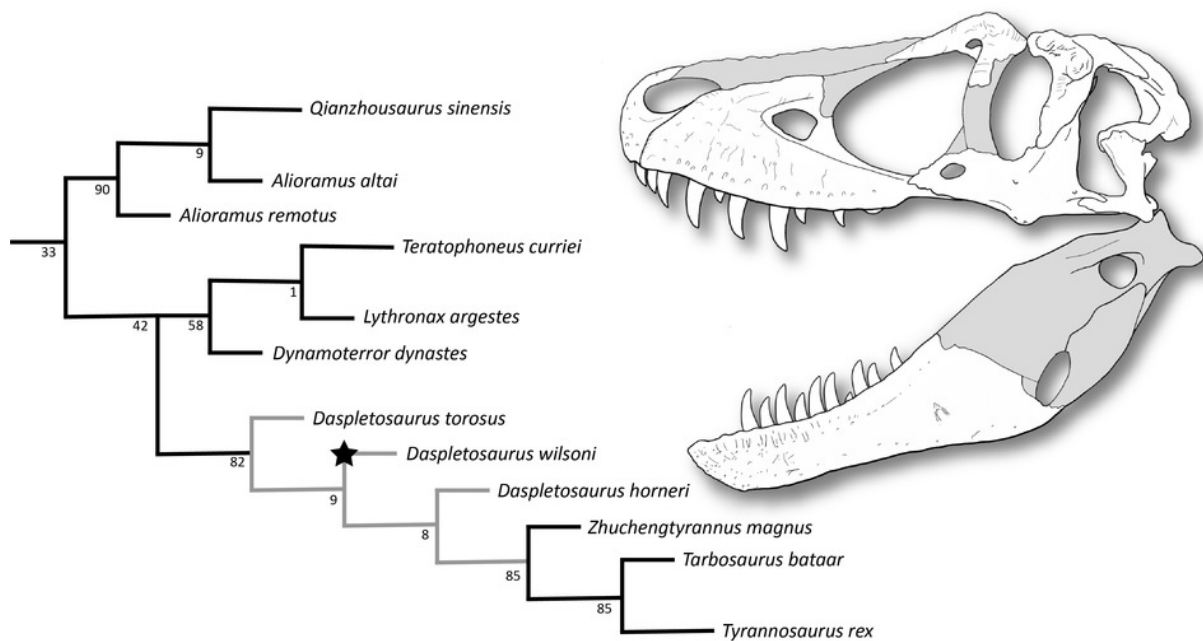


Figure 13

Time-calibrated phylogeny of *Daspletosaurus*.

Ages (left) are in Ma and are based on Carr et al. (2017) and Fowler (2017) for *D. torosus* and *D. horneri*. Representative skulls are, from top to bottom: *D. horneri*, MOR 590; *D. wilsoni*, BDM 107 (known material in white); *D. torosus*, CMN 8506. Star represents the temporal position of the *D. wilsoni* holotype (BDM 107; see Geologic Context) along an anagenetic *Daspletosaurus* lineage. Accompanying characters represent synapomorphies of progressively more exclusive clades represented by each taxon (e.g., *D. wilsoni* + more derived tyrannosaurines, *D. horneri* + more derived tyrannosaurines). No clear demarcations are drawn between taxa along the depicted lineage, given the relative paucity of specimens and the subjectivity intrinsic to species delineations of anagenetic lineages; ages of taxa are therefore imprecise. Scale is 10 cm.

